

1 **AMT-2020-383 - Response to Reviewer Comments and Manuscript Revisions**

2 **Reviewer 1 Comments – Responses and Manuscript Revisions**

3 **General comments.**

4 This paper uses measurements in highly concentrated fire plumes (within 100m of wildland grass fires,
5 and in controlled burns at the Missoula Fire Lab) to assess interferences in UV absorption measurements
6 of ozone at 254 nm.

7 This paper is motivated by the ozone measurements of UV absorption instruments, and the health impacts
8 from that ozone. Large increases in ozone may be observed after precursor NO_x and VOC have had time
9 to react. The time scale to produce that ozone is highly dependent on plume dilution, which itself is highly
10 variable in time, but typically takes place over hours since emission. A fundamental question: for direct
11 emissions, the interfering species will also be diluted, such that the lowest interferences may be expected
12 at the highest levels of plume ozone. Secondary production of UV-active hydrocarbons, e.g., production
13 of nitroaromatics following oxidation in the presence of NO₂, may dominate the ozone interference
14 downwind. What balance of directly emitted vs. secondary species are conjectured to lead to interferences
15 in ambient ozone measurements? Regardless of the source of the interference (primary vs. secondary),
16 given the lack of consistency from fire to fire (or even between different implementations of the UV
17 absorption technique) in the level of interferences measured, can the authors say what level of "fire
18 impact" causes a non-negligible interference? Is 1 ppm of ozone acceptable? 10 ppm of ozone?
19 Regardless, despite the experimental detail in this paper, it is not clear what ozone monitoring locations
20 are expected to suffer from significant interferences as a result of wildfires or prescribed burns. Lacking
21 these considerations, the paper's conclusions are qualitative at best, and by implication condemn a much
22 larger portion of the U.S. ozone monitoring network during the fire season than I suspect is warranted.
23 For a given UV absorption monitor, can they recommend what data to retain, and what data to eliminate
24 because of fire impacts? Some additional clarity in the real-world effects of fire smoke on ozone
25 monitoring is needed for this to make a novel and useful contribution to the literature.

26 The paper is overly long and can be shortened by removing extraneous details, repetitive text, and tables
27 that do not provide any usefully generalizable data as suggested below. Earlier literature is not well cited,
28 and additional references are also suggested below.

29 **Response:** The authors appreciate the time required to provide the review and feel that the suggestions
30 provided by the reviewer will result in an improved manuscript for resubmission.

31 The authors do agree that a more detailed look at data collected at sites being impacted by aged smoke
32 (ex. State and local regulatory monitoring sites being impacted by nearby wildfires and long range
33 transport of photochemically aged smoke plumes) and are currently collecting this data as part of the EPA
34 MASIC study in Boise, ID; Missoula, MT; and Reno, NV. This additional data collection will aid in
35 linking these research chamber and near field prescribed grassland burn measurements back to real world

36 regulatory monitoring situations. We will address these issues in a new “implications” section prior to
37 the manuscript conclusion.

38 The authors will, as suggested by the reviewer, attempt to shorten the length of the manuscript by
39 removing text that is tangential to the scope of the paper. In addition, the authors will review earlier
40 literature and cite as appropriate including those references suggested by the reviewer.

41 **Manuscript Revision:** The authors, as suggested by the reviewer removed text from the manuscript to
42 shorten the length of the document. An additional “Implications” section was added prior to the
43 conclusions section to tie the results of the research detailed in this manuscript to real world monitoring
44 applications. Included in this section will be a review of data from monitoring sites downwind of fires to
45 show the impact of the measurement artifacts described in this manuscript.

46

47 **Specific comments.**

48 **line 14:** "... large increases in ozone are also observed downwind ..." Is this always true?

49 **Response:** The authors did not imply that large increases in ozone are always observed down wind of
50 wildfire events. To clarify this and prevent assumptions that these increases in ozone “always occur”, the
51 text will be rewritten to include a statement like "... large increases in ozone have been observed
52 downwind ..."

53 **Manuscript Revision:** text changed to read "... large increases in ozone have been observed downwind
54 ..."

55 **line 32 (and lines 38 and 182 and elsewhere):** The NO-induced chemiluminescence measurement of
56 ozone is repeatedly described as "interference-free", which is misleading - it has a known dependency on
57 water vapor, which can lead to sensitivity variations of up to 8% if not accounted for. Please rephrase.

58 **Response:** The authors will rephrase these statements to emphasize that sample treatment steps, including
59 the use of a drier, must be taken prior to analysis to remove the effects of water vapor.

60 **Manuscript Revision:** Removed “interference free” from line 32. Removed “interference free” from
61 line 38. Clarifying statement inserted in line 62 “Both the ET-CL and NO-CL methods are subject to slight
62 interferences by water vapor. However, these potential interferences can be eliminated through the use of
63 Nafion based drier or equivalent sample water vapor treatment system.” Removed “interference free”
64 from line 182.

65 **line 52:** for clarity, please change to "... generates nitrogen dioxide in an electronically excited state..."
66 The original citation is Clough and Thrush, 1966, Chemical Communications, 728, pp. 783-784.

67 **Response:** The authors agree with this suggestion and will change the text accordingly.

68 **Manuscript Revision:** Text changed to read "... generates nitrogen dioxide in an electronically excited
69 state..."

70 **line 93:** please remove CO₂, as its absorption is negligible at 254 nm.

71 **Response:** The authors agree with this suggestion and will remove CO₂ from the text accordingly.

72 **Manuscript Revision:** CO₂ removed from the text

73 **line 142:** "...a supply of NO gas..." is not always needed - line 213 refers to one implementation of the
74 "scrubberless" UV absorption method uses a supply of N₂O gas and produces NO by photolysis.

75 **Response:** The authors agree with this suggestion and to clarify will rewrite the sentence to read: "The
76 SL-UV method requires a continuous supply of compressed NO or nitrous oxide (N₂O) (which the
77 instrument converts to NO) to serve as the scrubber gas.

78 **Manuscript Revision:** Sentence rewritten to read "Similar to NO-CL, the SL-UV method requires a
79 continuous supply of compressed NO or nitrous oxide (N₂O) (which the instrument converts to NO) to
80 serve as the scrubber gas.

81 **lines 230 - 237:** Details of power, generator, charger, and batteries are tangential to the performance of
82 the analyzers and could be eliminated to shorten the text.

83 **Response:** The authors agree with this suggestion and will review the manuscript and eliminate non-
84 relevant text that will shorten the document.

85 **Manuscript Revision:** Details of power, generator, charger, and batteries and other non-relevant material
86 removed from the manuscript text.

87 **lines 267-8:** "...calibrations for THC were performed using... a methane/propane gas cylinder..." This
88 work eventually concludes that VOCs are "likely to interfere with UV absorption measurements of O₃",
89 no surprise there. What is surprising is the rudimentary approach to quantifying those VOCs in this
90 manuscript. FID response factors vary with carbon number (for example, by up to a factor of 3 between
91 methane and propane!), between aliphatic, aromatic, and cyclic structures, and with heteroatomic
92 functionality. A sentence noting the uncertainty introduced in their measurement of VOCs (here called
93 THC) by using only methane and propane to determine FID sensitivity would be appropriate here.

94 **Response:** The authors agree with this comment and will add a sentence to address the uncertainty
95 associated with our use of the THC method and its calibration procedure to approximate VOC
96 concentrations.

97 **Manuscript Revision:** The THC calibration text was rewritten as follows to emphasize that the THC
98 results are an approximation of THC concentration in smoke "Per the manufacturer provided operators
99 manual, calibrations for THC were performed using the T700U calibrator and a certified EPA
100 methane/propane gas cylinder (Airgas). FID response factors for organic compounds can vary
101 significantly based upon factors such as carbon number and compound class (Tong and Karasek 1984).
102 The carbon numbers for methane and propane vary by a factor of three and the FID response factors for
103 those compounds may also vary by a similar amount. In addition, the complex mixture of hydrocarbons
104 found in smoke will have large variations in carbon number and FID response factors. As such, the results
105 obtained with the THC analyzer are an approximation of THC (and VOC) concentrations in smoke. In

106 addition, for THC calibrations, the T701H zero air generator was replaced with scientific grade zero air
107 compressed gas cylinders (Airgas).”

108 **Figure 2:** This is not a good graphic. There is absolutely no information conveyed by the third dimension
109 of this graph; please turn this into a 2D bar graph and improve the legibility of the different hatches. The
110 high level of interference from the UV-C and UVC- H techniques overwhelms any useful information on
111 the other techniques - suggest plotting only to 50 ppb and annotating the UV-C maxima with text. These
112 data are presented as O3 in ppb - what is the correct, or expectation value? The NO-CL data are lost in
113 this presentation and should be emphasized as the correct value.

114 **Response:** The authors agree the reviewers comment. The figure will be reformatted into 2D and
115 assuming that AMT allows colored figures will include a color scheme to improve clarity and viewability.
116 In addition, the y axis scale will be reduced to 50 ppb and the average values for all methods will be
117 included in the figure as text. The figure caption will be revised to reflect these changes.

118 **Manuscript Revision:** Figure 2 was reformatted into 2D and a color scheme added to improve
119 viewability. The y-axis scale was capped at 50 ppb and the average values for all methods and study
120 periods were included as text in the figure.

121 **Figure 4:** The NO-CL reference trace in the upper figure is the hardest to see; these figures could use
122 some work for legibility. The text refers to positive artifacts for the UV methods during burning periods,
123 ascribed to interferences from VOCs and PM2.5. Another problematic feature is the negative artifact
124 when the chamber is flushed with outside air, where the UV-C method falls below the NO-CL method
125 (bottom panel). Why is that? Did I miss the explanation?

126 **Response:** The authors will work on this time series as well as others to make the figures more legible
127 including looking into using a different scale on the y-axis. The post burn calibration checks on April 23,
128 2018 revealed a +8 % bias in the NO-CL method and a -2 % bias in the UV-C-H method. These biases
129 were evident during the chamber flush periods on that day. Each analyzer was re-zeroed and spanned
130 resulting in the elimination of the bias between the two methods as observed in the results from the
131 subsequent day (April 24, 2018). This will be addressed in the figure caption.

132 **Manuscript Revision:** Figure 4 was reformatted to include a logarithmic scale for O3 concentrations
133 making comparisons between the different methods more clear. The following text was added to the figure
134 caption to address the bias observed during the chamber flush periods “The post burn calibration checks
135 on April 23, 2018 revealed a +8 % bias in the NO-CL method and a -2 % bias in the UV-C-H method.
136 These biases were evident during the chamber flush periods on that day. Each analyzer was re-zeroed and
137 spanned resulting in the elimination of the bias between the two methods as observed in the results from
138 the subsequent day (April 24, 2018).”

139 **Lines 378-388:** I could not follow the confusing thread discussing how and when the MnO2 scrubber
140 failed in these experiments - for clarity I'd recommend deleting this section and removing all data taken
141 with an inoperative scrubber.

142 **Response:** The scope of this paper is a comparison/evaluation of ozone monitoring methods in smoke
143 and the damage to the converter occurred while operating the UV-C analyzer in heavy smoke, the authors
144 feel that this potential measurement issue is very important to those utilizing these instruments and should
145 at a minimum be mentioned in this manuscript. The converter issue is important in that the effect
146 continuous long after the smoke exposure is over and is not obvious when conducting typical QA/QC
147 reviews (e.g., zero/span calibrations and checks). The authors will add/remove text to clarify when the
148 damage occurred and the impact that the damaged converter had on the results obtained with the UV-C
149 method.

150 **Manuscript Revision:** The authors clarified some text in this section but feel the section is well explained
151 as to when the damage occurred and the overall impact. The section now reads “During the 2018 chamber
152 burns the UV-C results were biased high by 15-20 ppb even during non-burn (i.e., overnight) periods as
153 evident in Fig. 4 (top panel) and Fig. S4. The initial hypothesis was that the bias was associated with high
154 chamber backgrounds of interfering species due to years of heavy burning in the chamber. However, it
155 was later discovered during a subsequent summer/fall 2018 ambient air study in North Carolina in the
156 absence of smoke, that sampling heavy smoke plumes during the fall 2017 prescribed grassland burns
157 irreversibly damaged the MnO₂ scrubber in the UV-C instrument. The effect of the bias was observed
158 mainly when sampling ambient air and not readily observed during routine calibration checks (zeroes and
159 spans) except for an increase in the time required to obtain stable zero and span values. During the
160 summer/fall 2018 North Carolina study and prior to the start of the 2019 chamber burns, a new MnO₂
161 scrubber was installed and resulted in a significant and immediate reduction of the observed high bias,
162 shown in Fig. 4 (bottom panel) and Fig. S5.”

163 **Table 3:** Since there appears to be very large fire-to-fire and technique-to-technique variability in the
164 interferences, with no consistent dependence on any of the variables measured, quantifying their precise
165 values in a table seems not very useful. I’m not sure what information this table provides; what
166 quantitative use is it? Recommend deleting.

167 **Response:** The authors disagree with this comment. Regardless of the burning conditions or techniques
168 used, artifacts in the UV photometric methods were observed and are presented in this table. The authors
169 intend to include Table 3 in the manuscript.

170 **Manuscript Revision:** None

171 **line 498:** This section recommends using Nafion dryers to minimize smoke interferences in UV
172 absorption ozone measurements. This begs the question - under what range of conditions does the use of
173 a Nafion dryer allow EPA to actually accept an ozone measurement by the UV absorption measurement?
174 Please discuss.

175 **Response:** This comment goes beyond the scope of this paper which is primarily focused
176 evaluation/comparison of ozone monitoring methods in smoke plumes. However, the authors intend to
177 include an additional implication section that will discuss the potential impact of our findings on real
178 world monitoring application at sites that might be impacted by nearby wildfire smoke plumes.

179 **Manuscript Revision:** An implication section was added immediately preceding the conclusion section
180 that discusses the potential impact of our findings on real world monitoring application at sites that might
181 be impacted by nearby wildfire smoke plumes.

182 **Table 4:** Same comment as for Table 3, above: "Since there appears to be very large fire-to-fire and
183 technique-to-technique variability in the interferences, with no consistent dependence on any of the
184 variables measured, quantifying their precise values in a table seems not very useful. I'm not sure what
185 information this table provides; what quantitative use is it? Recommend deleting."

186 **Response:** The authors disagree with this comment. Regardless of the burning conditions or techniques
187 used, artifacts in the UV photometric method were observed and those artifacts are correlated with makers
188 of combustion as illustrated in this table. The authors intend to include Table 4 in the manuscript.

189 **Manuscript Revision:** None

190 **line 581:** I would suggest the authors review and cite the use of perfluorosulfonate membrane tubing to
191 remove UV-active hydrocarbons, e.g., in SO₂ pulsed fluorescence instruments (Luke, W., 1997, JGR,
192 102, 16,255-16,265).

193 **Response:** The authors will review the suggested manuscript and if appropriate cite in the text as a
194 possible solution in mitigating interferences by wildfire generated UV-active hydrocarbons as suggested
195 by the reviewer.

196 **Manuscript Revision:** None. The authors reviewed the suggested manuscript and choose not to cite it
197 in this manuscript. The authors could not find mention of perfluorosulfonate membrane in the manuscript
198 which is similar to the make up of Nafion but did notice several instances of the proprietary "kicker" that
199 may or may not remove interfering hydrocarbons.

200

201 **Reviewer 2 Comments – Responsenses and Manuscript Revisions**

202 **General Comments:** .

203 This study compares O₃ measurement techniques in fresh, concentrate smoke plumes. The authors sample
204 smoke plumes from both prescribed prairie grass burns and controlled chamber burns using a NO
205 chemiluminescence measurement as the interference-free standard with which to compare several
206 iterations of UV absorption-based measurements. This study is motivated by the prevalence of UV-based
207 O₃ analyzers at EPA air quality monitoring stations and the increasing impact of fire emissions on local
208 and regional air quality. Although these comparisons provide insight into the potential for UV-active
209 VOCs in smoke plumes to generate positive artifacts in the UV-based O₃ measurements, a more
210 quantitative assessment is limited by the lack of detailed VOC measurements and the inability to
211 quantitatively disentangle the various CO-O₃ regimes. The authors also suggest the role of Nafion in
212 mitigating potential artifacts, but do not provide enough information on the relative humidity conditions
213 during the various sampling periods or the potential for interactions between water vapor and VOC.
214 Further, the analysis emphasizes the effects of VOC interferences in near-fire smoke plumes but does

215 not provide much discussion on how the potential for interference diminishes with plume age and
216 dispersion. For example, how quickly do VOC react/diffuse to the point where their levels are no longer
217 of concern? How many ozone monitoring sites would be practically affected by these interferences?

218 **Response:** The authors appreciate the time required to provide the review and feel that the suggestions
219 provided by the reviewer will result in an improved manuscript for resubmission.

220 During both the prescribed and chamber burns, data were obtained for RH values and water vapor
221 concentration and is included in the data associated with this paper that will be provided through the EPA
222 Science Hub Web site (<https://catalog.data.gov/dataset/epa-sciencehub>) following the acceptance of this
223 paper. . However the correlations between RH and the magnitude of the ozone artifact were not
224 significant and therefore not included in the manuscript. In general, both the prescribed fire and chamber
225 burns were conducted under dry conditions with $RH \leq 50\%$. Past studies, which are now referenced in the
226 updated manuscript indicate that at those RH values humidity effects are expected to have little to no
227 impact. It is the intention of the authors to add an additional section to this manuscript discussing
228 implications of this research on real world ozone monitoring such as that that occurs at State and local
229 monitoring sites. The authors intend to review data from sites downwind of wildfires that potentially show
230 the artifact in the UV-C O₃ method and how it is correlated with markers of combustion processes. As
231 stated in the text of the manuscript, the authors plan future studies to dig deeper into the hypothesized
232 VOC caused artifact and which will include, as the reviewer suggest looking into interaction between
233 VOCs and water vapor and the capabilities of Nafion in removing certain VOCs.

234 **Manuscript Revision:** An additional “Implications” section was added prior to the conclusions section
235 to tie the results of the research detailed in this manuscript to real world monitoring applications. Included
236 in this section will be a review of data from monitoring sites downwind of fires to show the impact of the
237 measurement artifacts described in this manuscript.

238

239 **Specific Comments:**

240 **L243-244:** Is there any dependence of the artifact magnitude on distance from the active fire line? How
241 quickly do the VOC react/diffuse to the point where their levels are no longer detectable as a positive
242 artifact? All the measurements presented are taken within ~100 m from the fires, but any data collected
243 from aged smoke would be a useful counterpoint.

244 **Response:** The authors did not look at the dependencies of the artifact magnitude on distance from the
245 active fire line. However, the authors do agree that a more detailed look at data collected at sites being
246 impacted by aged smoke (ex. State and local monitoring sites being impacted by nearby wildfires). This
247 would aid in tying these measurements made in or near plume back to real world monitoring situations.
248 Most likely this will be done by adding an implications section prior to the manuscript conclusion.

249 **Manuscript Revision:** An implications section was added prior to the conclusion to address some of
250 reviewer 2 comments.

251 **L262:** The authors mention a +/- 10% performance objective between analyzers. Do the calibrations
252 reveal any systematic offset between the CL and UV analyzers? In describing the prescribed and chamber
253 burns, the authors mention varying moisture content in the burn material. Did the authors observe whether
254 the wetter grasses produced more VOC (lower combustion efficiency) in any systematic way?

255 **Response:** The calibrations only revealed a significant offset during one period during this study. The
256 post burn calibration checks on April 23, 2018 revealed a +8 % bias in the NO-CL method and a -2 %
257 bias in the UV-C-H method. These biases were evident during the chamber flush periods on that day.
258 Each analyzer was re-zeroed and spanned resulting in the elimination of the bias between the two methods
259 as observed in the results from the subsequen day (April 24, 2018). All other calibrations did not reveal
260 any systematic offsets or biases between the different analyzers and we will clarify this in the updated
261 version of the manuscript. At present the authors have not investigated the relationship between fuel
262 moisture content and VOC production. In order to simulate a range of natural burning conditions, the
263 chamber burns manipulated the moisture content, fuel type (pine needles, pine needles + fine woody
264 debris), and bulk density of the fuelbeds. These fuelbed properties influence the relative mix of flaming
265 and smoldering combustion and the chamber burns covered a range of combustion efficiencies (modified
266 combustion efficiencies of 0.85 – 0.97). The authors will investigate further and address these findings in
267 a future manuscript.

268 **Manuscript Revision:** The following text was added to the figure caption to address the bias observed
269 during the chamber flush periods “The post burn calibration checks on April 23, 2018 revealed a +8 %
270 bias in the NO-CL method and a -2 % bias in the UV-C-H method. These biases were evident during the
271 chamber flush periods on that day. Each analyzer was re-zeroed and spanned resulting in the elimination
272 of the bias between the two methods as observed in the results from the subsequen day (April 24, 2018).”

273 The following text was also added to section 3.2 “The post burn calibration checks on April 23, 2018
274 revealed a +8 % bias in the NO-CL method and a -2 % bias in the UV-C-H method. These biases were
275 evident during the chamber flush periods on that day. Each analyzer was re-zeroed and spanned resulting
276 in the elimination of the bias between the two methods as observed in the results from the subsequen day
277 (April 24, 2018).” No other calibration corrections werer made during the 2018 and 2019 chamber
278 studies.”

279 **Figure 4:** In general, the scale mismatch on the O3 timeseries makes immediate comparison between
280 methods difficult. The authors should perhaps switch to a log-scale on the y-axis that can effectively
281 compare low and high concentrations and offsets in both smoke plumes and background air. The authors
282 attempt to explain the positive offset of the UV-C method outside of the burning period, but there is also
283 a significant negative offset in the UV-C-H method that is not discussed. Could the authors provide more
284 insight on why the UV-C-H and NO-CL techniques disagree in background air?

285 **Response:** The authors will work on this time series plot as well as others to make the figures more legible
286 including looking into using a different scale on the y-axis. As suggested by the reviewer, the authors will
287 provide more insight into why the UV-C-H and NO-CL techniques disagree in background air.

288 **Manuscript Revision:** Figure 4 was reformatted to include a logarithmic scale for O₃ concentrations
289 making comparisons between the different methods more clear.

290 **L378+:** If the damaged MnO₂ scrubber ineffectively removed O₃, I would expect the UV-C measurement
291 to be biased low in background air rather than high. Please elaborate on the mechanism of MnO₂ damage
292 resulting in a significant positive offset. Also, it's unclear when the scrubber damage became an issue.
293 Did it affect data from the 2017 prescribed burns?

294 **Response:** In order for the scrubber to work correctly, it must remove O₃ and only O₃. Based upon the
295 data, the damage most likely resulted in the scrubber also removing significant amounts of interfering
296 species during the reference measurement which would then be detected as ozone during the sample
297 measurement resulting in the positive artifact. The data collected during the 2017 prescribed burns
298 indicate that the scrubber was functioning properly in that there was excellent agreement between the
299 UV-C and NO-CL methods when sampling out of the smoke plume.

300 **Manuscript Revision:** To clarify the section describing the bias observed during the 2018 chamber
301 studies was re-written as follows: "During the 2018 chamber burns the UV-C results were biased high by
302 15-20 ppb even during non-burn (i.e., overnight) periods as evident in Fig. 4 (top panel) and Fig. S4. The
303 initial hypothesis was that the bias was associated with high chamber backgrounds of interfering species
304 due to years of heavy burning in the chamber. However, it was later discovered during a subsequent
305 summer/fall 2018 ambient air study in North Carolina in the absence of smoke, that sampling heavy
306 smoke plumes during the fall 2017 prescribed grassland burns followed by subsequent storage of the UV-
307 C analyzer, irreversibly damaged the MnO₂ scrubber in the UV-C instrument. It is hypothesized that the
308 damage resulted in the scrubber removing some of the interfering species in addition to ozone, preventing
309 them from being removed in the reference measurement, and subsequent detection as ozone (positive bias)
310 during the measurement cycle. The effect of the bias was observed mainly when sampling
311 ambient/chamber air and not readily observed during routine calibration checks (zeroes and spans) except
312 for an increase in the time required to obtain stable zero and span values. The bias was not observed
313 during any of the 2017 prescribed grassland burns. During the summer/fall 2018 North Carolina study
314 and prior to the start of the 2019 chamber burns, a new MnO₂ scrubber was installed and resulted in a
315 significant and immediate reduction of the observed high bias, shown in Fig. 4 (bottom panel) and Fig.
316 S5."

317 **Figure S9** indicates there is potential artifact even <1-2 ppm CO. Do these plots just use data from the
318 burn periods or include points when chamber is flushed with outside air?

319 **Response:** Figure S9 includes data from the burn periods only. In the figure caption it describes it as "in-
320 plume". The authors will add clarifying text similar to the following, "...and THC for all in-plume (burn
321 period only) measurements...".

322 **Manuscript Revision:** The figure caption was re-written as follows: "Scatter plots between FRM and
323 FEM O₃ differences and CO, NO₂, and THC for all in-plume (burn period only) measurements made
324 during the 2018 and 2019 Missoula Fire Chamber studies. Observation points have been colored by the
325 O₃ instrument. Over all observations there is little correlation between the O₃ instrument differences,

326 but straight line structures within the overall scatters indicate that individual burn events measured in
327 the chamber have good correlations with distinct ratios.”

328 **L459-461:** How does the residence time and sample rate vary for each instrument?

329 **Response:** Sampling rates and hence residence times are going to be similar for all instruments as they
330 all operate with similar flow rates. The authors will address this comment by either adding analyzer flow
331 rate to Table 1 or by inserting text in the Methods section under each corresponding analyzer type.
332 Generally, UV photometric type analyzers require a greater flow rate because the flow is split between
333 the two cells (reference and measurement). The NO-CL method has only a single cell and requires a much
334 smaller flow rate to achieve a similar residence time.

335 **Manuscript Revision:** The flow rates of each method along with manufacturer reported performance
336 specifications were included in Table S1 which was added to the supplementary materials document. In
337 the text describing each method, a sentence similar to the following was added “Manufacturer provided
338 performance specifications for the NO-CL based TAPI T265 are given in Table S1.”

339 **Table 4:** The slope and intercept uncertainties should be included with the fit parameters. How different
340 are the range of fitted slope values statistically? In general, there is lack of uncertainty treatment in the
341 paper. How do the uncertainties compare for each measurement technique? This information should be
342 included in the manuscript.

343 **Response:** The authors agree with this comment and will work to include uncertainties (both in tables
344 and in the text) of measurement methods and in fit parameters associated with regression statistics.

345 **Manuscript Revision:** Data for the Konza March 2017 were re-analyzed and new values included for
346 slope, intercept R² and n. The previous analysis included a few values that were associated with CO
347 levels that were below 1 ppm (our threshold of sampling in plume). Standard errors for the regression
348 slope and intercept were included in Table 4. In addition, the following text was added to discuss the
349 results of the regression analysis between markers of combustion CO and THC and the magnitude of the
350 ozone artifact: “The slight differences in the magnitude of the artifacts (fitted regression slopes) along
351 with the low uncertainty (standard errors) values indicate that the magnitude of the artifact may be
352 influenced by local conditions that make each burn unique. Such conditions might include meteorological
353 conditions, fuel composition, fuel moisture content, and times spent in combustion phase (flaming vs
354 smoldering).”

355 **L550-552:** See question 1 above. How close to the plume do you have to be for interferences to matter?
356 Is this relevant for air quality monitoring stations not located in the immediate vicinity of the fire line?

357 **Response:** The authors focused on determining if significant ozone measurement artifacts do occur in
358 near-field smoke events and did not look at the dependencies of the artifact magnitude as a function of
359 distance from the active fire line. However the authors do agree that a more detailed look at data collected
360 at sites being impacted by aged smoke (ex. State and local monitoring sites being impacted by nearby
361 wildfires) and are currently collecting this data as part of the EPA MASIC study in Boise, ID; Missoula,
362 MT; and Reno, NV. This additional data collection will aid in linking these research chamber and near

363 field prescribed grassland burn measurements back to real world regulatory monitoring situations. We
364 will address these issues in a new “implications” section prior to the manuscript conclusion.

365 **Manuscript Revision:** An implications section was added to the manuscript prior to the conclusion to
366 address this and other comments provided by reviewer 2.

367 **L554:** What is estimated CO- Δ O₃ correlation for the chamber studies? It would still be worthwhile to
368 include this information in the supplement.

369 **Response:** Regarding the correlation between Δ O₃ and CO from the chamber based burns, the authors
370 refer the reviewer to the original manuscript text:

371 “As indicated, Δ O₃(UV-C) and CO appear to be correlated in time but when performing linear regression
372 comparisons of Δ O₃(UV-C) and CO during each years chamber burns as a whole, correlations tend to be
373 poor. We suspect the positive O₃ bias is driven by one or more VOCs (likely oxygenated VOCs). In fresh
374 smoke the excess concentrations of individual VOCs (Δ X), and VOC sums (Δ VOC), tend to be highly
375 correlated with Δ CO (Yokelson et al., 1999; Gilman et al. 2015). The emission ratios of individual VOCs
376 to CO (Δ X/ Δ CO) can vary considerably with combustion conditions such as fuel type and condition (e.g.
377 moisture content and decay state), fuel bed properties, such as bulk density, and the relative mix of
378 flaming and smoldering combustion (Gilman et al. 2015; Koss et al., 2017). Additionally, the response
379 of Δ X/ Δ CO to burn conditions varies among VOCs. When each burn is considered individually or in
380 groups with similar conditions, the correlations between Δ O₃, CO, and THC are enhanced. An example
381 of this behavior is shown in Supplementary Fig. S10.”

382 With that being stated, the authors will consider adding the CO- Δ O₃ correlation (both for the entire
383 chamber study period and also a subset of individual burns) either in Table 4 or in the body of the text
384 give evidence to the above statement. Visual representations of the correlations are given in Figures S9
385 and S10.

386 **Manuscript Revision:** The following text was added to section 3.4 to address this comment: “For the
387 chamber burns the magnitude of the ozone artifacts in ppb apparent O₃ per ppm CO, ranges between 6 -
388 210 ppb ppm⁻¹ for the individual burns. R² and standard error values were consistent with those observed
389 during the prescribed burns (see Table 4). “ In addition, the requested information is provided visually in
390 figures S9 and S10.

391 **Figures S9 and S10:** Can you demonstrably separate CO- Δ O₃ regimes based on “burn condition”? The
392 authors allude to this in the text (L563) and show an individual burn in Fig S10, but a more in-depth
393 analysis of the contributing burn condition factors would provide a more quantitative and perhaps
394 predictive assessment of how CO links to O₃ artifacts under the varied burn conditions. The authors also
395 perform separate regressions for NO₂ and THC, but a separate correlation with humidity might be
396 illustrative (if the data exists).

397 **Response:** The authors will consider elaborating further per the reviewers suggestion on CO- Δ O₃
398 regimes based on burn conditions (i.e., individual burns or burns grouped by similar burn conditions).
399 The authors previously attempted to establish a correlation between Δ O₃ and humidity (water vapor

400 concentration) but those correlation were extremely poor. As such the authors chose not to include this
401 analysis.

402 **Manuscript Revision:** The following text was added to section 3.4 to elaborate on the lack of correlation
403 between ΔO_3 and CO when considered as a whole but showing improvements when considering
404 individual burns: “For the chamber burns the magnitude of the ozone artifacts in ppb apparent O_3 per ppm
405 CO, ranges between 6 - 210 ppb ppm⁻¹ for the individual burns. R^2 and standard error values were
406 consistent with those observed during the prescribed burns (see Table 4).”

407 **L571:** Is it possible that interactions between water vapor and VOC somehow compound the VOC effect?
408 In other studies (e.g., Spicer et al. 2010, Turnipseed et al. 2017), Nafion alone seems to play little role in
409 mitigating VOC artifacts but does significantly reduce water vapor artifacts. In drier environments, does
410 adding Nafion affect the positive artifact magnitude? This would be more conclusive evidence that Nafion
411 does in fact remove certain permeable VOC species.

412 **Response:** Both the 2017 prescribed fire and 2018-2019 chamber based burns were conducted under dry
413 conditions ($RH \leq 50\%$) and humidity interferences are expected to be minimal. As stated in the previous
414 comment, the correlation between in plume water vapor concentration and ΔO_3 was not significant. In
415 addition, there is no significant correlation between the magnitude of the artifact and RH. In both the
416 prescribed grassland and chamber burns there was a UV instrument with a Nafion drier and a UV
417 instrument without the drier and they were operated simultaneously. The magnitude of the artifact (both
418 average and maximum) was greatly reduced in the method using the Nafion drier. This is evident in
419 comparing the magnitude of the UV-C artifact with that of the UV-C-H (UV method employing a Nafion
420 based drying system. In all cases, the UV-C artifact was nearly an order of magnitude greater than that of
421 the UV-C-H. This is also became further evident when the Nafion drier was added to the UV-C method
422 on the final day of burning during the 2018 chamber studies, thus reducing the magnitude of the UV-C
423 artifact to a point comparable to that of the UV-C-H method. The effect of Nafion on the magnitude of
424 the artifact is detailed in section 3.3. In section 3.5 of the manuscript, the authors will attempt to clarify
425 that in addition to our hypothesis of certain VOCs being removed by the Nafion, there may also be
426 interactions between water vapor and VOCs that may be confounding the observed artifact.

427 **Manuscript Revision:** The authors feel that text and discussion provided in section 3.3 already provide
428 a response to the reviewer 2's comment suggestion. As stated in the response listed above, during this
429 study humidity effects are expected to be at a minimum due to the low RH values that existed during all
430 study periods. As such and to clarify, the following text was inserted in section 2.6: “In general, chamber
431 RH values were below 50% facilitating dry burning condition.” And section 3.1: “In addition, ambient
432 RH values were generally below 50% indicating that the spring and fall 2017 prescribed burns were
433 conducted under dry conditions.”

434 The last sentence of section 3.4 was re-written to read “Considering that the prescribed grassland and
435 chamber burns were conducted under dry conditions, the size of the difference (as large as hundreds of
436 ppb) cannot be explained purely by the previously observed relative humidity effects on measurements
437 (Leston et al., 2005; Wilson et al., 2006), suggesting that the Nafion® dryer is directly impacting the
438 concentrations of other interferences in the sample stream.”

439 **L605:** Could this also be confounded by the faulty MnO₂ scrubber?

440 **Response:** We do know that during the 2018 chamber studies the damaged scrubber did cause an
441 approximate +10-15 ppb bias in the UV-C method which was present even in the absence of smoke. At
442 the end of the 2018 chamber studies, the authors added a Nafion drier to the UV-C method as indicated
443 in Figure 4. The addition of the Nafion to the UV-C method reduced the magnitude of the artifact by a
444 factor of three making it compatible to the artifact observed for the UV C-U method. The addition of the
445 nafion did result in a slight reduction in the bias that we attributed to damaged scrubber but not on the
446 order of 3X. We suspect that the addition of the drier would reduce or remove many of the VOC species
447 prior to also being removed by the faulty scrubber thus resulting in a reduction of the bias but not
448 completely eliminating it. The authors will add clarifying text in the body of the manuscript explaining
449 the damage to the MnO₂ scrubber and its hypothesized effect on the observed bias. The reviewers
450 comment would only apply to the 2018 chamber study as the MnO₂ scrubber in the UV-C method was
451 functioning properly during all other studies.

452 **Manuscript Revision:** Clarifying text was added in section 3.2 to explain the effect that the damaged
453 scrubber had on the UV-C ozone results (positive bias).

454

455 **Technical Corrections:**

456 **Table 1:** Add uncertainty associated with each measurement technique. Sample rate would also be useful.

457 **Response:** The authors will address this comment by either adding analyzer flow rate and uncertainties
458 to table 1 or by inserting text in the Methods section under each corresponding analyzer type.

459 **Manuscript Revision:** An additional table (Table S1) was added to the supplemental materials document
460 containing manufacturer provided performance specifications for each analyzer to address this comment
461 from reviewer 2. In the text describing each method, a sentence similar to the following was added
462 “Manufacturer provided performance specifications for the NO-CL based TAPI T265 are given in Table
463 S1.

464 **Figure S1 and other timeseries in general:** It’s difficult to compare NO-CL and UV measurements of
465 plumes and background air given the large mis-match in scale. Some other way of presenting this material
466 (e.g., semi-log) might help the visual comparison. The lines are also not very easy to distinguish. Using
467 different colors instead of just patterns would help.

468 **Response:** The authors agree with this comment and will take steps to improve the the time series plots,
469 including looking into different scales (e.g. semi-log) and also using colored lines in the figures.

470 **Manuscript Revision:** Figures 4 and S1-5 were reformatted adding logarithmic scales where appropriate
471 and color schemes to improve readability.

472 **Figure 2:** Does not need to be in 3D and could use a color scheme instead of patterns.

473 **Response:** The authors agree with the reviewers comment. The figure will be reformatted into 2D and
474 assuming that AMT allows colored figures will include a color scheme to improve clarity and view ability.
475 In addition, the y axis scale will be reduced to 50 ppb and the average values for all methods will be
476 included in the figure as text. The figure caption will be revised to reflect these changes.

477 **Manuscript Revision:** Figure 2 was reformatted into 2D and a color scheme added to improve
478 viewability. The y-axis scale was capped at 50 ppb and the average values for all methods and study
479 periods were included as text in the figure.

1 **Comparison of Ozone Measurement Methods in Biomass Burning Smoke: An evaluation under**
2 **field and laboratory conditions**

3 Russell W. Long¹, Andrew Whitehill¹, Andrew Habel², Shawn Urbanski³, Hannah Halliday¹, Maribel Colón¹, Surender
4 Kaushik¹, Matthew S. Landis¹

5 ¹Center for Environmental Measurement and Modeling, Office of Research and Development, United States Environmental
6 Protection Agency, Research Triangle Park, North Carolina, United States of America

7 ²Jacobs Technology Inc., Research Triangle Park, North Carolina, United States of America

8 ³U.S. Forest Service, Rocky Mountain Research Station, Missoula, MT, United States of America

9

10 *Correspondence to:* Russell W. Long (long.russell@epa.gov; (919) 541-7744)

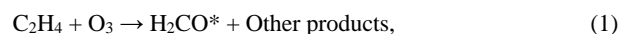
11 **Abstract**

12 In recent years wildland fires in the United States have had significant impacts on local and regional air
13 quality and negative human health outcomes. Although the primary health concerns from wildland fires
14 come from fine particulate matter (PM_{2.5}), large increases in ozone (O₃) ~~are also~~have been observed
15 downwind of wildland fire plumes ([DeBell et al., 2004](#); [Bytnerowicz et al., 2010](#); [Preisler et al.,](#)
16 [2010](#); [Jaffe et al., 2012](#); [Bytnerowicz et al., 2013](#); [Jaffe et al., 2013](#); [Lu et al., 2016](#); [Lindaas et al., 2017](#);
17 [McClure and Jaffe, 2018](#); [Liu et al 2018](#); [Baylon et al., 2018](#); [Buysse et al. 2019](#)). Conditions generated
18 in and around wildland fire plumes, including the presence of interfering chemical species, can make the
19 accurate measurement of O₃ concentrations using the ultraviolet (UV) photometric method challenging if
20 not impossible. UV photometric method instruments are prone to interferences by volatile organic
21 compounds (VOCs) that are present at high concentrations in wildland fire smoke. Four different O₃
22 measurement methodologies were deployed in a mobile sampling platform downwind of active prescribed
23 grassland fire lines in Kansas and Oregon and during controlled chamber burns at the United States Forest
24 Service, Rocky Mountain Research Station Fire Sciences Laboratory in Missoula, Montana. We
25 demonstrate that the Federal Reference Method (FRM) nitric oxide (NO) chemiluminescence monitors
26 and Federal Equivalent Method (FEM) gas-phase (NO) chemical scrubber UV photometric O₃ monitors
27 are relatively interference-free, even in near-field combustion plumes. In contrast, FEM UV photometric
28 O₃ monitors using solid-phase catalytic scrubbers show positive artifacts that are positively correlated
29 with carbon monoxide (CO) and total gas phase hydrocarbons (THC), two indicator species of biomass

30 burning. Of the two catalytic scrubber UV photometric methods evaluated, the instruments that included
31 a Nafion® tube dryer in the sample introduction system had artifacts an order of magnitude smaller than
32 the instrument with no humidity correction. We hypothesize that Nafion®--permeable VOCs (such as
33 aromatic hydrocarbons) could be a significant source of interference for catalytic scrubber UV
34 photometric O₃ monitors, and that the inclusion of a Nafion® tube dryer assists with the mitigation of
35 these interferences. The ~~interference-free~~ chemiluminescence FRM method is highly recommended for
36 accurate measurements of O₃ in wildland fire plume studies and at regulatory ambient monitoring sites
37 frequently impacted by wildland fire smoke.

38 **1 Introduction**

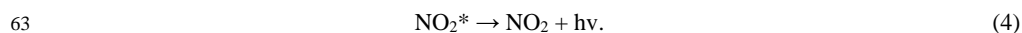
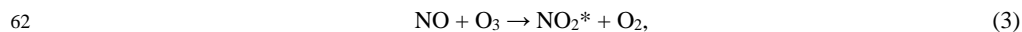
39 Ground-level ozone (O₃) is a secondary air pollutant generated from the photochemical interactions of
40 nitrogen oxides (NO_x) and volatile organic compounds (VOCs). The most robust methods for
41 ~~interference-free~~ O₃ measurements are based on chemiluminescence reactions with ethylene (ET-CL, for
42 ethylene chemiluminescence) or nitric oxide (NO-CL, for nitric oxide chemiluminescence) (Long et al.,
43 2014). The overall reaction mechanism for ET-CL generally proceeds as detailed in Eqs. (1-2):



46
47
48 The reaction generates electronically-activated formaldehyde (H₂CO*) which luminesces in the high
49 ultraviolet (UV) to visible portion of the spectrum (380 nm - 550 nm) and vibrationally-activated
50 hydroxide ions which luminesce in the visible light to the low infrared (IR) portion of the spectrum (550
51 nm - 800 nm). The number of photons emitted during the reaction is directly proportional to the amount
52 of O₃ present and are counted by a photomultiplier tube (PMT), with its response centered at 440 nm,
53 then the count is converted to O₃ concentration. The ET-CL method requires a constant supply of ethylene
54 for continuous operation. NO-chemiluminescence analyzers measure O₃ concentrations using the
55 principle that the dry, gas-phase reaction between NO and O₃ generates nitrogen dioxide in an
56 electronically excited state~~generates nitrogen dioxide in an activated state~~ (NO₂*), and oxygen (O₂)

57 (Ollison et. al., 2013; Boylan et.al., 2014). As each unstable, NO₂* molecule returns to a lower energy
58 state (NO₂), it emits a photon (hv). The reaction causes luminescence in a broadband spectrum ranging
59 from visible light to infrared light (approximately 590 nm – 2800 nm). The two-step gas-phase reaction
60 proceeds as detailed in Eqs. (3-4):

61



64

65 The ET-CL method is no longer used nor produced commercially and has been replaced by the NO-CL
66 method. Similar to the ET-CL method, the NO-CL method requires a constant supply of gas, in this case
67 NO, for continuous operation. Both the ET-CL and NO-CL methods are subject to slight interferences by
68 water vapor. However, these potential interferences can be eliminated through the use of Nafion based drier
69 or equivalent sample water vapor treatment system. The ET-CL method was promulgated as the Federal
70 Reference Method (FRM) for measuring O₃ in the atmosphere in 1971 and the NO-CL method
71 promulgated as the FRM in 2015 (U.S. EPA, 2015).

72

73 While the chemiluminescence method for measuring O₃ is technically robust and free of analytical
74 artifacts (Long et al., 2014), it is not widely used in the United States. Instead, Federal Equivalent Methods
75 (FEM) based upon UV photometry are employed at the majority of O₃ regulatory monitoring locations.
76 According to July 2020 data from the United States Environmental Protection Agency (EPA) Air Quality
77 System (AQS) database, the UV photometric method represents 99% of the roughly 1200 instruments
78 deployed in network monitoring for O₃ National Ambient Air Quality Standard (NAAQS) attainment.
79 UV photometric methods for O₃ are generally considered easier to deploy, operate, and in most cases do
80 not require external compressed gasses for operation. UV photometric analyzers determine O₃
81 concentrations by quantitatively measuring the attenuation of light due to absorption by O₃ present in an
82 absorption cell at the specific wavelength of 254 nm (Parrish et al., 2000; Williams et al., 2006). The O₃
83 concentration is determined through a two-step process in which the light intensity passing through the
84 sample air (I) is compared with the light intensity passing through similar sample air from which all O₃

85 is first removed (I_0). The ratio of these two light intensity values (I/I_0) provides the measure of the light
86 absorbed at 254 nm, and the O_3 concentration in the sample is then determined through the use of the
87 Beer-Lambert Law as given in Eq. (5):

$$I/I_0 = e^{-KLC} \quad (C = 1/KL \ln [I/I_0]); \quad (5)$$

88
89
90
91 where L is the length of the absorption cell (cm), C is the O_3 concentration (ppm), and K is the absorption
92 cross section of O_3 at 254 nm at standard atmospheric temperature and pressure conditions ($308 \text{ atm}^{-1} \text{ cm}^{-1}$)
93 ¹). Photometric monitors generally use mercury vapor lamps as the UV light source, with optical filters
94 to attenuate lamp output at other than the 254 nm wavelength.

95
96 Air for the reference cell measurement (I_0) is typically obtained by passing the ambient air sample stream
97 through a catalytic scrubber containing manganese dioxide (MnO_2), hopcalite (a mixture of Cu, Mn, and
98 Ag oxides), heated silver wool, or another solid state material to ‘scrub’ only O_3 from the sample air while
99 preserving all other substances in the sample air that potentially absorb at 254 nm (e.g., elemental gaseous
100 mercury [Hg^0], hydrogen, sulfide [H_2S], ~~carbon dioxide [CO_2]~~, VOCs) so that their effects are cancelled
101 in the differential I/I_0 measurement. The integrity of the O_3 reference scrubber is critical and may allow
102 measurement interferences if it does not perform adequately. Similarly, any tendency of the scrubber to
103 fail to effectively remove all O_3 from the reference sample will result in a measurement bias. In addition
104 to O_3 , catalytic scrubbers have been shown to remove UV-active VOCs (Kleindienst et al., 1993), creating
105 the potential for positive artifacts in O_3 measurements when the efficiency of this VOC removal is
106 impacted.

107
108 Although FEM designated UV photometric instruments are accurate under most ambient conditions,
109 locations with high VOC concentrations can produce significant analytical artifacts. Smoke plume
110 impacted locations and measurements downwind from wildland fires are a particular concern; O_3
111 measurements of up to 320 ppb were observed in a smoke plume in western Oregon using a Dasibi
112 1003AH UV photometric O_3 monitor (Huntzicker and Johnson, 1979), which also showed a correlation

113 between apparent O₃ and aerosol concentrations (**b_{scat}**, a combustion plume indicator in this case). O₃
114 measurements from UV photometric instruments exceeding 1500 ppb at night (22:00-05:00) were
115 observed in Fort McMurray, Alberta during smoke impacts from the 2016 Horse River Fire, which were
116 positively correlated with NO and non-methane hydrocarbons (Landis et al., 2018). Follow-up pyrolysis
117 experiments demonstrated that ET-CL instruments do not show a similar response to biomass burning
118 smoke (Huntzicker and Johnson, 1979). Photochemical chamber experiments comparing the O₃ response
119 of UV (Dasibi Model 1003AH, Dasibi Model 1008AH, and Thermo Model 49) and ET-CL (Bendix
120 Model 8002 and Monitor Labs Model 8410) mixtures show negligible differences for irradiated
121 paraffin/NO_x and olefin/NO_x mixtures, but do show a positive UV interference in mixtures with toluene
122 and other aromatics present (Kleindienst et al., 1993). Laboratory studies comparing the response of UV
123 (Thermo Model 49, Horiba APOA-370, and 2B Tech Model 202) and ET-CL (Bendix) instruments
124 showed a positive interference for o-nitrophenol, naphthalene, and p-tolualdehyde for the UV instruments
125 but not the ET-CL instruments (Grosjean and Harrison, 1985; Spicer et al., 2010). Additionally, during
126 the Mexico City Metropolitan Area field campaign (MCMA-2003) a mobile laboratory using an FEM
127 designated UV photometric O₃ monitor (unheated MnO₂ scrubber, Thermo 49 series) showed a large
128 positive O₃ interference (~400 ppb) associated with PM_{2.5} and polyaromatic hydrocarbons (PAHs) when
129 following some diesel vehicles (Dunlea et al., 2006). Although not compared to a chemiluminescence
130 instrument, those high O₃ values are unlikely real considering the high concurrent NO concentrations (in
131 some cases, >1000 ppb). The authors of this study attributed the interference to fine particles, based on
132 the correlation with PM_{2.5} and the lack of a correlation with gas-phase organic species measured by the
133 proton transfer reaction-mass spectrometer (PTR-MS, Dunlea et al., 2006).

134

135 In addition to interferences from the presence of aromatic VOCs and semi-volatile PAHs, water vapor
136 (relative humidity) issues have also been observed with older generation FRM and FEM designated
137 chemiluminescence and UV photometric O₃ instruments, respectively (Kleindienst et al., 1993; Leston
138 et al., 2005; Wilson and Birks, 2006). As such, Nafion[®] tube dryers are regularly incorporated into some
139 newer generation chemiluminescence and UV photometric O₃ monitors in an attempt to mitigate the
140 humidity related measurement artifacts.

141

142 A recently introduced variation of the UV photometric method, known as the “scrubberless” UV
143 photometric (SL-UV) method (Ollison et al., 2013), specifies removal of O₃ from the sample air for the
144 reference by a gas-phase reaction with NO rather than using a conventional solid state catalytic scrubber.
145 The NO gas phase chemical scrubber reacts with O₃ much faster and more selectively than with other
146 potential interfering compounds and is very effective at removing the O₃ without affecting other
147 interfering compounds that may be present in ambient air. The differential UV measurement can then
148 effectively reduce interferences to an insignificant level. Similar to NO-CL, the SL-UV method requires
149 a continuous supply of compressed NO or nitrous oxide (N₂O) (which the instrument converts to NO) to
150 serve as the scrubber gas. ~~Similar to NO-CL, the SL-UV method requires a supply of NO gas for~~
151 ~~continuous operation.~~

152

153 In this study, we investigate UV photometric FEM instrument O₃ measurement interferences in fresh
154 biomass burning smoke plumes from prescribed grassland fires and during controlled burn experiments
155 in a large scale combustion chamber. We directly compare NO-CL FRM O₃ measurements to several
156 FEM designated UV photometric technologies, including a gas-phase scrubber and catalytic scrubbers
157 with and without Nafion[®] tube dryer systems. Based on the results from the measurements, we assess the
158 magnitude of the observed artifacts for different technologies and under various smoke conditions and
159 provide suggestions for potential mitigation of the interferences.

160

161 2. Methods

162 2.1 Overview of Methods Evaluated

163 In this study we compared the measurement results from six different commercially available FRM/FEM
164 designated O₃ instruments operated in ambient or chamber generated biomass burning smoke. All
165 instruments were operated according to their FRM or FEM designation. The six instruments differed by
166 measurement principle (chemiluminescence *versus* UV photometric), and by sample treatment

167 configuration (scrubber material, presence of dryer, etc.). For interference free O₃ measurements we
 168 utilized the newly designated FRM NO-CL method (U.S. EPA, 2015). For the UV photometric methods,
 169 we compared both catalytic scrubber and “scrubberless” (gas phase chemical scrubber) technologies, with
 170 the “scrubberless” monitor using a NO chemical scrubber. Finally, within the catalytic scrubber UV
 171 photometric category, we compared instruments with and without Nafion tube dryer systems. The
 172 operation principle and designations (FRM vs FEM) for the analyzers under investigation are summarized
 173 in Table 1 and described in Sections 2.1.1-2.1.4. These analyzers were operated immediately downwind
 174 of fresh biomass burning plumes during eight days of prescribed fires in grassland ecosystems in Oregon
 175 and Kansas and during laboratory-based studies at the U.S. Forest Service’s (USFS) combustion facility
 176 at the Fire Sciences Laboratory (FSL) in Missoula, Montana. The grassland fire fuels consisted primarily
 177 of mixed native prairie tall grass of varying moisture content. Seven of the eight days of prescribed
 178 burning were conducted in the Tallgrass Prairie ecosystem of central Kansas (four days in March of 2017
 179 and three days in November of 2017). The additional burn day was conducted at the Sycan Marsh in
 180 central Oregon (October of 2017). Laboratory based chamber burns at the FSL were conducted during
 181 April 2018 and again during April 2019. Fuels for the laboratory based chamber burns consisted of
 182 ponderosa pine needles and fine woody debris. Details of the individual studies are provided in Sections
 183 2.2-2.6.

184

185 **Table 1: Ozone measurement methods investigated.**

Name	Manufacturer	Model	Method	Scrubber	Cells	Humidity Correction	Deployment ^a
U.S. EPA Federal Reference Methods (FRM)							
NO-CL	Teledyne API	T-265	CL (NO)	N/A	1	Nafion [®] -based (dryer)	K1, S, K2, T, M1, M2
U.S. EPA Federal equivalent methods (FEM)							
UV-C	Thermo Scientific	49i	UV (254 nm)	Catalyst (MnO ₂)	2	None	K1, S, K2, T, M1, M2
UV-C-H	2B Technologies	205	UV (254 nm)	Catalyst (Hopcalite)	2	Nafion [®] -based (equilibration)	K1, S, K2, T, M1
SL-UV	2B Technologies	211	UV (254 nm)	Gas chemical (NO)	2	Nafion [®] -based (equilibration)	K1, M1, M2
UV-G	2B Technologies	211-G	UV (254 nm)	Heated graphite	2	Nafion [®] -based (equilibration)	M2

186 ^aK1-Konza Prairie March 2017; S-Sycan Marsh, October 2017; K2-Konza Prairie November 2017; T-Tallgrass Prairie
 187 November 2017; M1-Missoula chamber April 2018; M2-Missoula chamber April 2019.

189 **2.1.1 NO Chemiluminescence**

190 The FRM O₃ measurement method was the ~~interference-free~~ Teledyne API (San Diego, CA, USA) Model
191 T265 Chemiluminescence Monitor (TAPI T265), which utilizes a NO-CL measurement principle. These
192 NO-CL O₃ analyzers have been shown to be free of interferences (Long et al. 2014) , and have been used
193 as a reference method in other O₃ comparison studies (Williams et al., 2006; Landis et al., 2020). Although
194 there is a known water vapor interference with chemiluminescence technology (Kleindienst et al., 1993),
195 the TAPI T265 uses a Nafion[®] tube dryer system to remove water vapor from the air prior to making the
196 measurement, thus eliminating any humidity-related effects. Like the ET-CL technologies (Kleindienst
197 et al., 1993), the NO-CL analyzers have no documented VOC interferences. [Manufacturer provided](#)
198 [performance specifications for the NO-CL based TAPI T265 are given in Table S1.](#)

199

200 **2.1.2 Catalytic Scrubber UV Photometric**

201 For this study the UV photometric method with no humidity correction was represented by the Thermo
202 Scientific (Franklin, MA, USA) Model 49i (Thermo 49i), which is a dual cell instrument with a
203 manganese oxide (MnO₂) catalytic scrubber, referred to as UV-C. Nafion[®]-based humidity systems or
204 dryers have been employed within photometric O₃ monitors with catalytic scrubbers before the
205 measurement cell, offering a reduction in relative humidity interferences and artifacts (Wilson and Birks,
206 2006). [Manufacturer provided performance specifications for the UV-C based Thermo 49i are given in](#)
207 [Table S1.](#)

208

209 The UV photometric with a Nafion[®] humidity conditioning system was represented in this study by a 2B
210 Technologies (Boulder, CO, USA) Model 205 (2B 205) O₃ monitor. The 2B 205 utilized a dual-cell
211 design where sample air and scrubbed air are measured simultaneously. The 2B 205 uses a Hopcalite
212 (CuO/MnO₂) catalytic scrubber to remove O₃ from the reference stream. This instrument will be referred

213 to as UV-C-H. [Manufacturer provided performance specifications for the UV-C-H based 2B 205 are](#)
214 [given in Table S1.](#)

215

216 **2.1.3 Scrubberless UV Photometric**

217 For comparison with the NO-CL, UV-C and UV-C-H methodologies, a “scrubberless” UV (SL-UV)
218 photometric analyzer with a gas-phase (NO) chemical scrubber was employed (Ollison et al., 2013;
219 Johnson et al., 2014). The addition of NO gas to the reference stream selectively scrubs O₃ while not
220 significantly affecting interfering VOC species, resulting in an interference free O₃ determination.
221 Inclusion of this instrument into the study allows evaluation of the impact of the UV method in general
222 (as compared with chemiluminescence) versus the influence of specific scrubber technologies. The SL-
223 UV method is represented by the 2B Technologies Model 211 “Scrubberless” Ozone Monitor (2B 211).
224 The Model 2B 211 requires a continuous supply of compressed NO or nitrous oxide (N₂O) (which the
225 instrument converts to NO). The SL-UV method also utilizes a Nafion[®]-based sample humidity
226 conditioning system to eliminate any humidity effects. The SL-UV instrument was not used in the October
227 or November 2017 burns due to the lack of the necessary reagent gas (nitrous oxide, N₂O) needed to run
228 the instrument. [Manufacturer provided performance specifications for the SI-UV based 2B 211 are given](#)
229 [in Table S1.](#)

230

231 **2.1.4 Heated Graphite Scrubber UV Photometric**

232 During the final phase of laboratory-based burning a 2B Technologies Model 211-G UV photometric
233 analyzer (2B 211-G) was operated for comparison to the monitors detailed in Sections 2.1.1-2.1.3. The
234 2B 211-G differs from the 2B 211 in that it employs a heated graphite scrubber to remove O₃ from the
235 reference sample stream (I₀) (Turnipseed et al., 2017). The 2B 211-G utilizes the same Nafion[®]-based
236 sample humidity conditioning system as employed in the 2B 211. For the purposes of this manuscript the
237 UV photometric method employing the heated graphite scrubber be referred to as UV-G. [Manufacturer](#)
238 [provided performance specifications for the UV-G based 2B 211-G are given in Table S1.](#)

240 2.2 Prescribed Fire Burn Mobile Sampling Platform

241 During the prescribed fire grass burns, all study instrumentation (analyzers, data acquisition systems, and
 242 peripheral systems) were mounted in portable instrument racks and installed inside an enclosed EPA 4x4
 243 vehicle (Whitehill et al., 2019). ~~During initial set up and in between burning periods instruments were
 244 powered via land line AC power routed through two onboard mounted Tripp Lite (Chicago, IL, USA)
 245 Model SMART3000RM2U 3000VA line interactive sine wave uninterrupter power supplies (UPS) each
 246 running off its own 20A circuit to ensure that the instruments had a stable supply of clean power.
 247 Immediately prior to deploying to the burns, the instruments were then switched to a bank of six 12V
 248 100Ah batteries run through an AIMS Power (Reno, NV, USA) model PICOGLF30W12V120V 3000W
 249 pure sine wave global low frequency inverter and charger located in a trailer towed behind the EPA
 250 vehicle. An on board 6500W Honda generator was used to maintain charge on the batteries.~~ The
 251 instruments were connected via perfluoroalkoxy alkane (PFA) Teflon[®] tubing (0.64 cm diameter) to PFA
 252 Teflon[®] filter packs loaded with 47 mm, 5 micron pore size pressure drop equivalent Millipore
 253 (Burlington, MA, USA) Omnipore[®] polytetrafluoroethylene (PTFE) filter membranes which were (i)
 254 mounted to a rooftop sampling platform during Spring 2017 sampling, or (ii) connected to a cross-linked
 255 Teflon[®]-coated high flow manifold mounted on the inside roof of the truck compartment during Fall 2017
 256 sampling. The truck was positioned downwind of active biomass burning plumes, usually within meters
 257 to hundreds of meters of the active fire line, and positioned so that the trailer was downwind of the sample
 258 inlets (to avoid interferences from generator exhaust). In addition to the O₃ analyzers under investigation,
 259 additional monitors were also operated for the determination of carbon monoxide (CO), NO, NO₂, total
 260 oxides of nitrogen (NO_x=NO+NO₂), and ~~total hydrocarbons (THC, to approximate VOC concentrations).~~
 261 The operation principle and designation (FRM vs FEM) information for the additional analyzers deployed
 262 in this study are summarized in Table 2. Data from all instruments was recorded on a Envivas Ultimate
 263 data acquisition system.

264

265 **Table 2: Additional measurement methods operated during the present study.**

Pollutant	Manufacturer	Model	Method	FRM/FEM	Deployment ^f
-----------	--------------	-------	--------	---------	-------------------------

CO	Teledyne API	48C	NDIR ^a	FRM	K1, S, K2, T, M1, M2
NO ₂	Teledyne API	T500U	CAPS ^b	FEM	K1, S, K2, T, M1, M2
NO, NO ₂ , NO _x	Thermo Scientific	42C	CL (O ₃) ^c	FRM	K1, K2, T, M1
NO, NO ₂ , NO _x	Teledyne API	T200/T201 ^e	CL (O ₃)	FRM	M1, M2
THC	Thermo Scientific	51i	FID ^d	NA	K2, T, M1, M2

266 ^aNon-Dispersive Infrared Absorption

267 ^bCavity Attenuated Phase Shift

268 ^cOzone Chemiluminescence

269 ^dFlame Ionization Detector

270 ^eThe Teledyne API Model T201 is not a designated FRM or FEM however it employs the same operating principle as the FRM designated model T200

272 ^fK1-Konza Prairie March 2017; S-Sycan Marsh October 2017; K2-Konza Prairie November 2017; T-Tallgrass Prairie November 2017; M1-Missoula chamber April 2018; M2-Missoula chamber April 2019.

274

275 All instruments were calibrated with multipoint calibrations before and after each sampling day. All pre-
276 and post-calibrations met our quality performance objectives of +/- 10% and linearity of $r^2 \geq 0.99$. For
277 the O₃ analyzers under investigation, field and laboratory calibrations were performed using a Teledyne
278 API Model T700U Dynamic Dilution Calibrator with a NIST traceable O₃ photometer and O₃ generation
279 system. Zero air for the calibrator was supplied by a Teledyne API Model T701H Zero Air Generator.
280 Calibrations for NO, NO₂, NO_x and CO were performed using the same calibrator and zero air generator
281 utilizing a certified EPA protocol tri-blend (CO, NO, SO₂) gas cylinder (Airgas). Per the manufacturer
282 provided operators manual, ~~C~~calibrations for THC were performed using the T700U calibrator and a
283 certified EPA methane/propane gas cylinder (Airgas). FID response factors for organic compounds can
284 vary significantly based upon factors such as carbon number and compound class (Tong and Karasek
285 1984). The carbon numbers for methane and propane vary by a factor of three and the FID response
286 factors for those compounds may also vary by as similar amount. In addition, the complex mixture of
287 hydrocarbons found in smoke will have large variations in carbon number and FID response factors. As
288 such, the results obtained with the THC analyzer are an approximation of THC (and VOC) concentrations
289 in smoke. In addition, for THC calibrations, the T701H zero air generator was replaced with scientific
290 grade zero air compressed gas cylinders (Airgas).

291

292 **2.3 Kansas Prescribed Burns, March 2017**

293 Biomass burning plumes were sampled during four days of prescribed burns (March 15-17, 2017 and
294 March 20, 2017) on the Konza Prairie Long Term Ecological Research (LTER) site outside of Manhattan,
295 Kansas. The fuels for this series of burns consisted of mixed native prairie tall grass of varying moisture
296 content. Over the four-day period, a total of 13 burns were conducted and sampled.

297

298 **2.4 Oregon Prescribed Burns, October 2017**

299 A single 10-hour day of prescribed grassland burning was measured at the Sycan Marsh Preserve in
300 central Oregon on October 11, 2017. Fuels for the Sycan Marsh burn consisted of mixed native prairie
301 tall grass of varying moisture content.

302

303 **2.5 Kansas Prescribed Burns, November 2017**

304 Biomass burning plumes were sampled during a single day of prescribed burning (November 10, 2017)
305 on the Konza Prairie LTER site outside of Manhattan, Kansas and on two additional days (November 13,
306 2017 and November 15, 2017) at the Tall Grass Prairie National Preserve outside Strong City, Kansas.
307 Fuels for the November 2017 burns consisted of mixed native prairie tall grass of varying moisture
308 content. During the November 10 sampling, two separate burns were conducted. Three burns were
309 conducted over the two days at Tallgrass Prairie.

310

311 **2.6 USFS Missoula Burn Chamber Burns 2018, 2019**

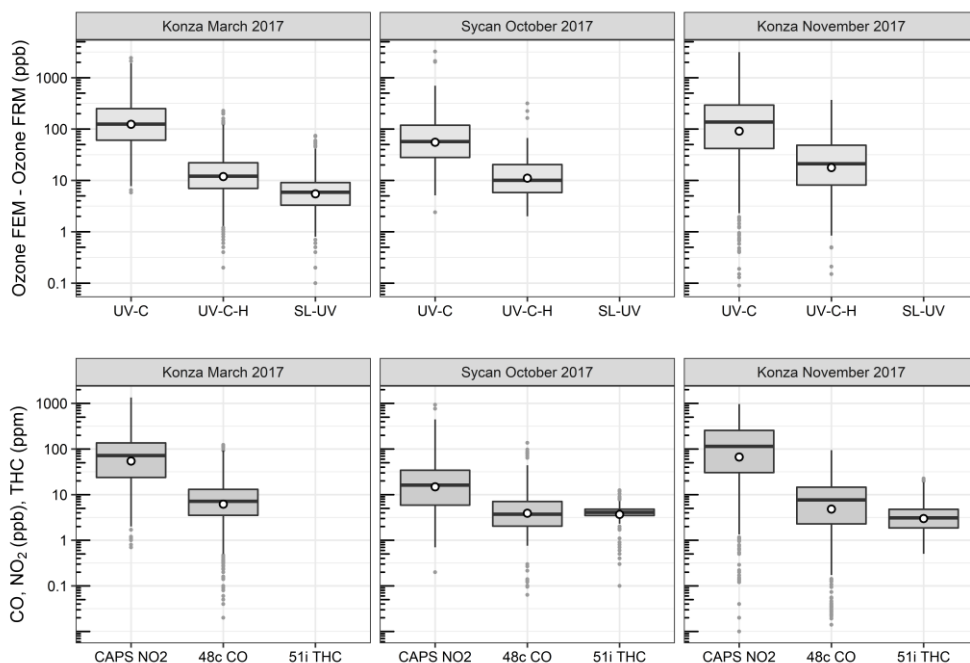
312 Laboratory-based studies were performed at the U.S. Forest Service's combustion testing facility at the
313 FSL in Missoula, Montana by EPA and USFS personnel. These static chamber burns occurred in the
314 spring of 2018 (April 16-24, 2018; 33 burns; Landis et al., 2020) and again in the spring of 2019 (April
315 15-26, 2019; 31 burns). The main combustion chamber is a square room with internal dimensions 12.4 x
316 12.4 x 19.6 m high and a total volume of 3000 m³ and has been described previously (Bertschi et al.,

317 2003; Christian et al., 2004; Yokelson et al., 1996; Landis et al., 2020). During the combustion chamber
318 studies, the facility was fitted with identical instrumentation racks, calibration systems, systems for
319 sampling of test atmosphere, and data acquisition systems, as those described in Section 2.2. All
320 instrumentation were housed in an observation room immediately adjacent to the combustion chamber
321 with PFA inlet lines extending through the wall into the chamber. All inlet lines contained an identical
322 filter pack/filter assembly described in Section 2.2 to protect inlet lines and the analyzers from particulate
323 contamination. Fuel beds consisting of ponderosa pine needles and mixed woody debris were prepared
324 and placed in the middle of chamber. The amount and moisture content of the fuels were varied to generate
325 different flaming/smoldering conditions during the burns. During the chamber burns the combustion room
326 was sealed and the fuel bed was ignited. Two large circulations fans on the chamber walls and one on the
327 ceiling facilitated mixing and assured homogeneous conditions during the burn periods (Landis et al.,
328 2020). In general, chamber RH values were below 50% facilitating dry burning condition.

329 **3 Results and Discussion**

330 **3.1 Results from Ozone Measurements in Prescribed Grassland Fire Plumes**

331 O₃ measurement results from the Oregon and Kansas prescribed grassland fires studies are shown as the
332 difference between the FEM and FRM in Fig. 1 and 1-minute average time series plots for the studies are
333 presented in Supplementary Figs. S1-S3. There were significant differences in the measurement results
334 obtained from the different O₃ monitors operated during the prescribed fires. The UV-C instrument
335 (Thermo 49i) consistently showed large increases in O₃ concentration readings in fresh biomass burning
336 plumes, with measurements exceeding the FRM measurement by 2-3 ppm. The O₃ exceedances were



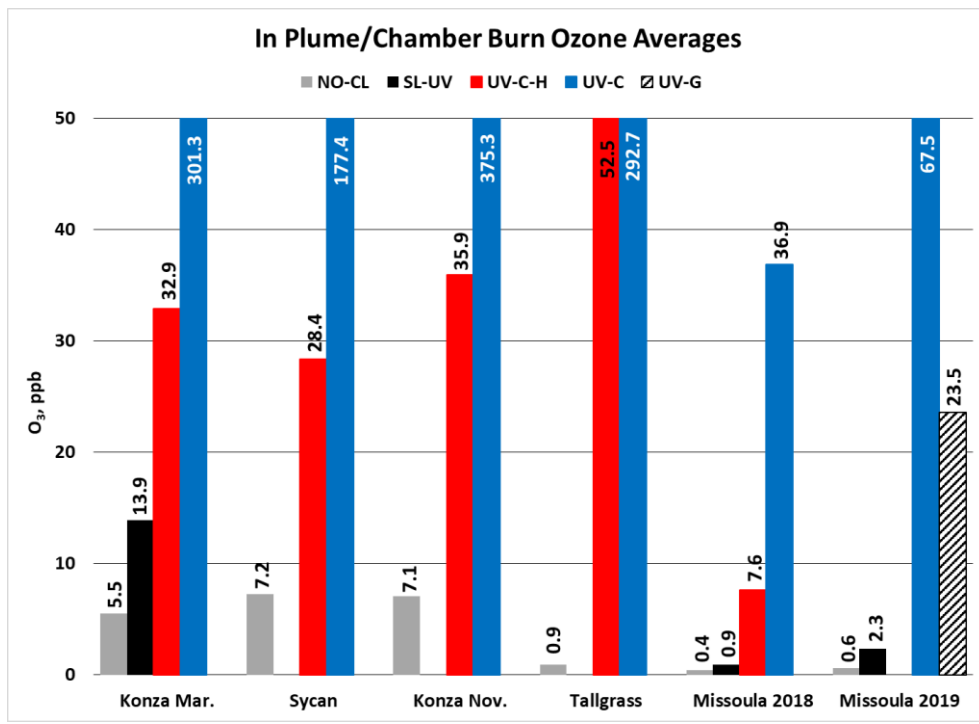
337

338 **Figure 1.** Ozone concentration differences between FEM instruments and the FRM instrument (FEM-
 339 FRM), and the measured NO₂, CO, and total hydrocarbons (THCs) during the three 2017 wildfire
 340 deployments. All measurements included are within-smoke only measurements, and show both the
 341 elevated smoke tracers (NO₂, CO, THC), and the persistent elevation of the FEM O₃ measurements. The
 342 box and whisker plots indicate the 25th, 50th, and 75th quartiles, with the whiskers extending to 1.5 times
 343 the inner quartile range. The open dots indicate the mean values for each instrument within smoke.

344

345 generally correlated in time with CO and THC (biomass burning indicators) and NO₂. These correlations
 346 will be discussed separately. The UV-C-H instrument (2B 205) also showed increased readings in smoke
 347 plumes (also correlated with CO, THC, and NO₂), but with absolute measurements roughly an order of
 348 magnitude smaller than the UV-C instruments. The NO-CL (T265) instrument results showed the
 349 opposite behavior, with reductions in O₃ readings inversely correlated with increases in NO₂

350 concentrations, as expected from general O₃ titration by NO (NO + O₃ → NO₂ + O₂). For the March 2017
 351 measurements the SL-UV instrument (2B 211) produced readings roughly comparable with the NO-CL
 352 monitor, but with substantially more noise on a minute-to-minute timescale. The “in plume” average O₃
 353 concentrations from the four prescribed grassland burning periods are shown in Fig. 2. For the purposes
 354 of this comparison, CO measurements were used as an indicator of when sampling occurred “in plume.”
 355 In addition, ambient RH values were generally below 50% indicating that the spring and fall 2017
 356 prescribed burns were conducted under dry conditions.

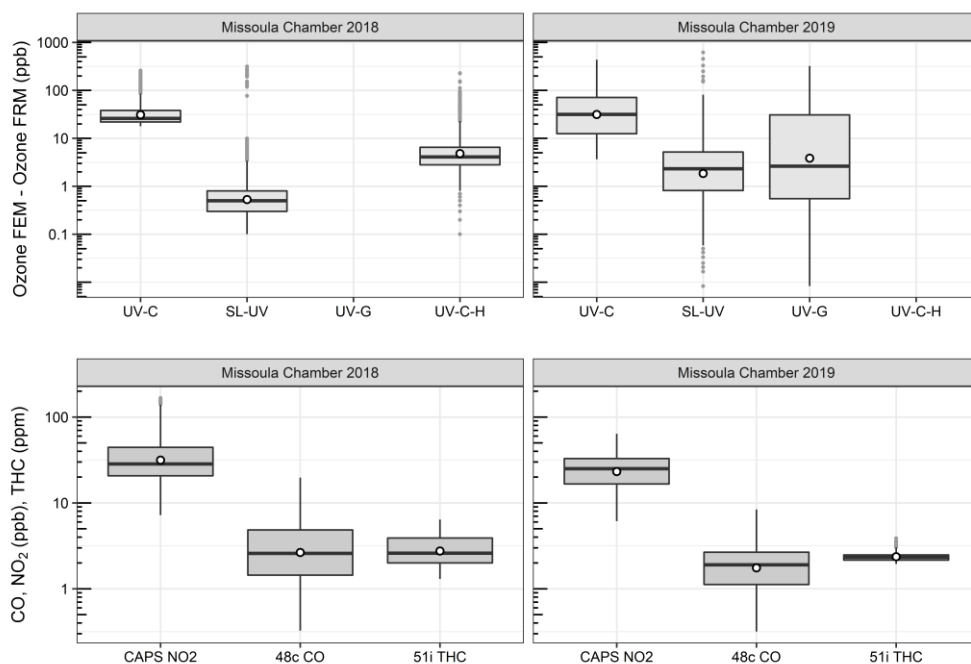


357
 358 **Figure 2.** In plume O₃ concentration averages from the 2017 prescribed grassland burns and the 2018 and
 359 2019 Missoula chamber burns. For the 2017 grassland burning periods, CO concentration results (≥1
 360 ppm) were used as an indicator of when “in-smoke” sampling was occurring.

361

362 3.2 Results from Ozone Measurements in USFS Chamber Burns

363 O₃ measurement results from the 2018 and 2019 USFS chamber burn studies are shown in Fig. 3. Time

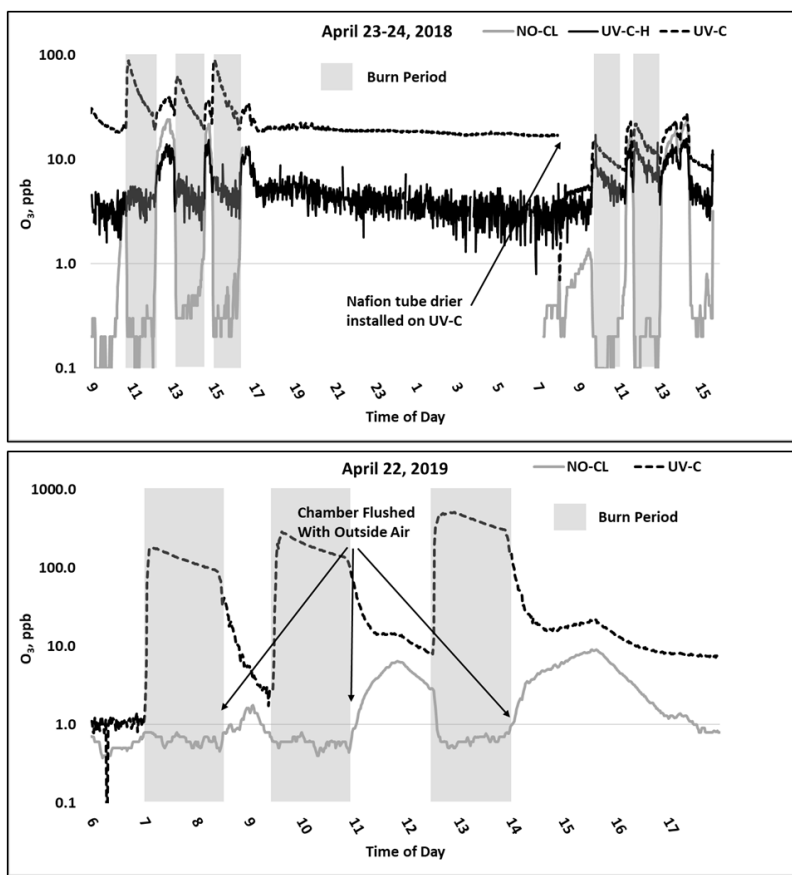


364

365 **Figure 3.** Differences between the FEM and FRM instrument concentrations (FEM-FRM), and NO₂,
366 CO, and total hydrocarbons (THCs) concentrations during the 2018 and 2019 Missoula chamber studies.
367 All measurements included are within-smoke only measurements, and show both the elevated smoke
368 tracers (NO₂, CO, THC), and the persistent elevation of the FEM O₃ measurements compared to the FRM.
369 The box and whisker plots indicate the 25th, 50th, and 75th quartiles, with the whiskers extending to 1.5
370 times the inner quartile range. The open dots indicate the mean values for each instrument within smoke.

371

372 series plots of the chamber Study data are included in Supplementary Figs. S4 and S5. Figure 4 gives a
373 more detailed view of UV-C and NO-CL O₃ results (two days from 2018 and one day from 2019) during



374

375 **Figure 4.** Time series example of USFS chamber burn O₃ results from the NO-CL, UV-C, and UV-C-H
376 (2018 only) from April 23-24, 2018 (top) and April 22, 2019 (bottom). O₃ concentrations are displayed
377 in a logarithmic scale. The post burn calibration checks on April 23, 2018 revealed a +8 % bias in the NO-
378 CL method and a -2 % bias in the UV-C-H method. These biases were evident during the chamber flush

Formatted: Subscript

379 periods on that day. Each analyzer was re-zeroed and spanned resulting in the elimination of the bias
380 between the two methods as observed in the results from the subsequen day (April 24, 2018).

381

382 the chamber burns. In contrast to the prescribed grassland burns, the Missoula chamber burns employed
383 differing fuel types (ponderosa pine needles and fine woody debris) that are more typical of fuels
384 consumed during western U.S. forest fires. In addition, the concentrations of pollutants generated and
385 observed during the chamber studies were approximately an order of magnitude smaller than those
386 observed during the prescribed grassland fires. For reference, maximum PM_{2.5} concentrations observed
387 during the prescribed fires were in excess of 50 mg m⁻³ while maximum chamber PM_{2.5} concentrations
388 were less than 2 mg m⁻³ range. Regardless of these differences, there were still significant (order of
389 magnitude or more) differences in the measurement results between the different FEM O₃ instruments
390 operated during both the 2018 and 2019 chamber studies. The NO-CL method showed identical trends to
391 those observed during the grassland burns in that its measured O₃ concentrations dropped to near zero
392 during the active burning periods as indicated in Fig. 4 (active burning periods shaded in grey). The only
393 periods when significant O₃ concentrations were measured by the NO-CL method was when outside air
394 was brought in to flush the chamber in between burns. The post burn calibration checks on April 23, 2018
395 revealed a +8 % bias in the NO-CL method and a -2 % bias in the UV-C-H method. These biases were
396 evident during the chamber flush periods on that day. Each analyzer was re-zeroed and spanned resulting
397 in the elimination of the bias between the two methods as observed in the results from the subsequen day
398 (April 24, 2018).” No other calibration corrections werer made during the 2018 and 2019 chamber
399 studies. As in the grassland fire plumes, the UV-C method showed increased O₃ concentration (positive
400 analytical artifact) readings that were correlated in time with CO and NO₂; See Supplementary Figs. S9
401 and S10. Similarly, the UV-C-H instrument also showed increased positive analytical artifacts during the
402 chamber burns, but with absolute measurement values about an order of magnitude smaller than the UV-
403 C instruments. The SL-UV method gave similar results to the NO-CL method during both the 2018 and
404 2019 chamber burns. Newly added during the 2019 burns, the UV-G method (2B 211-G) gave mixed
405 results: at times it provided similar results compared to the NO-CL and SL-UV methods, and at others it
406 provided results in line with those provided by the UV-C method. See Supplementary Fig. S5 for the 2019

407 chamber burn time series plot. The burn average O₃ concentrations from the 2018 and 2019 chamber
408 burns are presented in Fig. 2.

409 During the 2018 chamber burns the UV-C results were biased high by 15-20 ppb even during non-burn
410 (i.e., overnight) periods as evident in Fig. 4 (top panel) and Fig. S4. The initial hypothesis was that the
411 bias was associated with high chamber backgrounds of interfering species due to years of heavy burning
412 in the chamber. However, it was later discovered during a subsequent summer/fall 2018 ambient air study
413 in North Carolina in the absence of smoke, that sampling heavy smoke plumes during the ~~spring and~~-fall
414 2017 prescribed grassland burns followed by subsequent storage of the UV-C analyzer, irreversibly
415 damaged the MnO₂ scrubber in the UV-C instrument. It is hypothesized that the damage resulted in the
416 scrubber removing some of the interfering species in addition to ozone, preventing them from being
417 subtracted off as background in the reference measurement, and subsequent detection as ozone (positive
418 bias) during the measurement cycle. The effect of the bias was observed mainly when sampling
419 ambient/~~chamber~~ air and not readily observed during routine calibration checks (zeroes and spans) except
420 for an increase in the time required to obtain stable zero and span values. The bias was not observed
421 during any of the 2017 prescribed grassland burns. During the summer/fall 2018 North Carolina study
422 and prior to the start of the 2019 chamber burns, a new MnO₂ scrubber was installed and resulted in a
423 significant and immediate reduction of the observed high bias, shown in Fig. 4 (bottom panel) and Fig.
424 S5.

425 **3.3 Methodological Influence on Ozone Measurements in Biomass Burning Smoke**

426 As discussed in Sections 3.1 and 3.2, there are large (order of magnitude level) differences in O₃
427 concentration measurement results obtained from the FRM (NO-CL) and the FEM UV photometric with
428 catalytic scrubber (UV-C) O₃ methods. The extremely low O₃ concentrations measured by the NO-CL
429 instrument is consistent with O₃ depletion in the presence of high NO_x concentrations (up to ppm levels)
430 observed in the grass burning plumes and during chamber burns. The reaction between NO and O₃ is
431 rapid and occurs on the timescales of seconds to minutes. As a result, high NO in the fresh biomass
432 combustion plumes will efficiently titrate out O₃ leading to near-field depletion within the plumes relative
433 to background concentrations. There was no sign of a positive interference in the NO-CL monitors, and

434 it remains the most robust and accurate routine method for O₃ measurement in fresh and downwind
435 biomass burning plumes.

436

437 In contrast with the NO-CL FRM instrument results, the UV-C FEM results showed substantial increases
438 in reported O₃ concentrations in the fresh biomass burning plumes. There is no known pathway for direct
439 O₃ emission from biomass burning, and the proximity (meters to hundreds of meters) and timescales
440 (seconds to minutes travel time from the combustion source to measurement) involved are too short for
441 the usual NO_x – VOC photochemistry to produce secondary O₃. Further, since the FSL chamber interior
442 is not exposed to sunlight, photochemistry would not have been active in the Missoula laboratory burns.
443 For the purposes of this work, the positive analytical artifact in the UV-C method, termed $\Delta O_{3(UV-C)}$, is
444 estimated using Eq. (6) as the difference between UV-C and the NO-CL O₃ concentration measurement
445 results for the same time period:

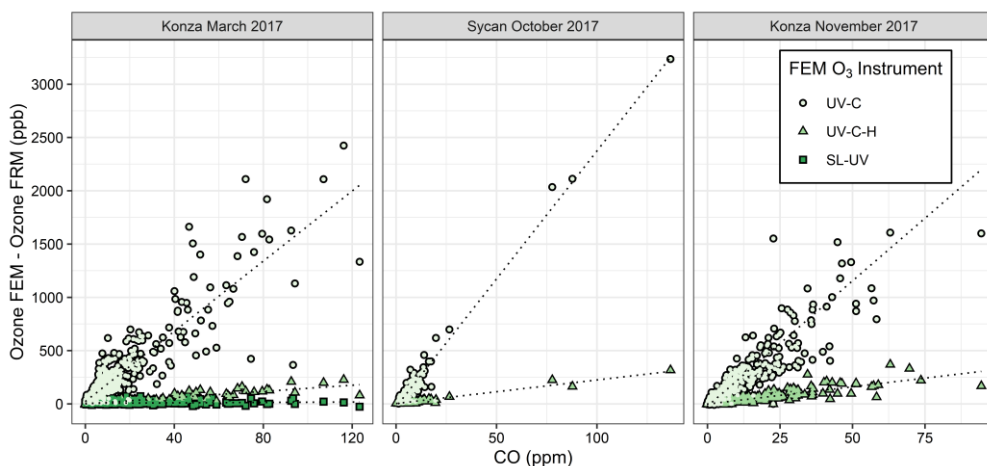
446

$$447 \quad \Delta O_{3(UV-C)} = UV-C - NO-CL \quad (6)$$

448

449 Figure 5 shows “in plume” regressions between $\Delta O_{3(UV-C)}$ and the FRM measurement and CO for the
450 three measured prescribed grassland burns in 2017 (Supplementary Fig. S6 shows the time series of
451 $\Delta O_{3(UV-C)}$ and CO). Figure 5 and Supplementary Fig. S6 show good correlations within the smoke plumes.
452 The average and maximum values of $\Delta O_{3(UV-C)}$ are summarized in Table 3. It is hypothesized that the
453 large “O₃” measurement observed in the UV-C method results from a positive interference or artifact,
454 likely linked to VOC emissions in the grassland burn plumes. VOCs are emitted in higher concentrations
455 from the smoldering phase of combustion, which is also characterized by large CO emissions (Yokelson
456 et al., 1996; Yokelson et al., 1997), so a correlation between CO and O₃ artifact would support the
457 hypothesis of a VOC-linked interference for the UV-C instruments. This is also consistent with observed
458 VOC interferences in previous studies (Grosjean and Harrison, 1985; Kleindienst et al., 1993; Spicer et
459 al., 2010) and observed following fireworks (Fiedrich et al., 2017; Xu et al., 2018).

460



461

462 **Figure 5.** Scatter plots between FEM and FRM O₃ differences and the CO measurements within the
 463 grassland fires smoke plumes. The FEM measurements are differentiated by color and shape. The SL-UV
 464 method was only run during the Konza March 2017 measurements.

465

466 **Table 3: Ozone artifact (ΔO_3) averages, maximum values, and CO, NO₂, and THC averages from
 467 the prescribed fire and USFS chamber burns as measured by the UV-C, UV-C-H, and UV-G
 468 instruments.**

Study	ΔO_3 avg. (ppb)	ΔO_3 max (ppb)	CO avg. (ppm)	NO ₂ avg. (ppb)	THC avg. (ppm)
ΔO_3(UV-C)					
Mar. 2017 Konza Prairie (KS)	295.8	2423.7	15.8	147.3	-
Oct. 2017 Sycan Marsh (OR)	170.2	3235.5	8.5	60.5	2.7
Nov. 2017 Konza & Tallgrass Prairies (KS)	330.0	3156	14.1	156.9	4.0
Apr. 2018 USFS Chamber (MT)	36.5	309.6	3.8	35.6	2.8
Apr. 2019 USFS Chamber (MT)	66.9	530.9	2.1	31.7	4.8
ΔO_3(UV-C-H)					
Mar. 2017 Konza Prairie (KS)	42.8	227.1	15.8	147.3	-
Oct. 2017 Sycan Marsh (OR)	21.1	316.4	8.5	60.5	2.7
Nov. 2017 Konza & Tallgrass Prairies (KS)	40.2	369.0	14.1	156.9	4.0
Apr. 2018 USFS Chamber (MT)	7.2	136.8	3.8	35.6	2.8
ΔO_3(UV-G)					
Apr. 2019 USFS Chamber (MT)	22.9	376.8	2.1	31.7	4.8

$\Delta O_3(\text{SL-UV})$					
Mar. 2017 Konza Prairie (KS)	8.3	74.2	15.8	147.3	-
Apr. 2018 USFS Chamber (MT)	0.5	11.5	3.8	35.6	2.8
Apr. 2019 USFS Chamber (MT)	1.7	32.1	2.1	31.7	4.8

469

470 The presence of a Nafion[®]-based humidity conditioning system (Nafion[®] tube dryer) significantly
471 reduced the magnitude of the observed artifact as evident by comparing the UV-C and UV-C-H results
472 shown in Figs. 1-3 and Supplementary Figs. S1 – S5. As with the UV-C method, the artifact in the UV-
473 C-H method, $\Delta O_{3(\text{UV-C-H})}$, is calculated using Eq. (7) as the difference between UV-C-H and the NO-CL
474 O₃ concentration measurement results for the same time period:

475

476

$$\Delta O_{3(\text{UV-C-H})} = \text{UV-C-H} - \text{NO-CL} \quad (7)$$

477

478 The addition of the Nafion[®]-based humidity conditioning system reduces the magnitude of the $\Delta O_{3(\text{UV-C-}}$
479 $\text{H})$ artifact by approximately an order of magnitude as compared with the UV-C method. This is further
480 illustrated in the 2018 chamber burns, where prior to beginning the final burn day on April 24, 2018, a
481 Nafion[®] tube dryer (PermaPure, MD Monotube Dryer Series) was installed on the UV-C method (Thermo
482 49i) in effect, converting it to a UV-C-H method. As shown in Fig. 4 and Supplementary Fig. S4, the
483 addition of the Nafion[®] tube dryer significantly reduced the $\Delta O_{3(\text{UV-C-H})}$ artifact to a point comparable with
484 that observed in the UV-C-H method (2B 205). A possible explanation for this effect is presented and
485 discussed in Section 3.5. In addition, the previously described bias related to the damaged MnO₂ scrubber
486 was also reduced upon addition of the Nafion[®] dryer to the UV-C method.

487

488 For the March 2017 Konza Prairie study (Fig. 1) and the 2018 and 2019 USFS chamber studies (Fig. 3)
489 the SL-UV instrument concentration results were comparable to, although noisier and slightly higher than,
490 the NO-CL reference instrument. On numerous occasions during the prescribed and chamber burns, the
491 SL-UV instrument shows short (i.e. one-minute data point) positive or negative excursions that are not
492 also observed in the NO-CL results. In addition, these excursions are not correlated with changes in CO
493 concentrations. Because the SL-UV is a dual cell instrument that measures O₃ by comparing the

494 absorbance of two cells, it is critical in highly dynamic environments (such as during this study) that both
495 cells be measuring the same air at the same time. A slight difference in flow rates or residence times
496 between the two pathways (or a delay in one pathway relative to the other) will cause short term variability
497 in the difference between the two cells. Although this does not pose an issue for longer time averaging
498 (i.e. hourly data) under stable conditions, the dynamic nature of biomass burning plumes (i.e. changing
499 on the order of seconds) and short time averages (i.e. minute) can create issues (noise) for the SL-UV
500 method.

501

502 Significant analytical artifacts were observed for FEM UV photometric O₃ instruments with (UV-C-H)
503 and without (UV-C) Nafion[®]-based humidity conditioning system, where it appears that the dual effect
504 of ambient humidity fluctuations and VOC interferences caused large positive over-measurement of “in-
505 smoke” O₃ concentrations. Chemiluminescence monitors are highly specific to O₃ and have long been
506 known to be free of VOC interferences (Long et al., 2014; U.S. EPA, 2015). However, studies have shown
507 that the chemiluminescence method can be impacted by changes in relative humidity (Kleindienst et al.,
508 1993). As such, upon promulgation in 2015, the new NO-CL FRM regulatory text requires a humidity
509 correction/dryer system to eliminate the potential water vapor interference. As configured from the
510 manufacturer, the NO-CL based Teledyne-API Model T265 instrument operated during this comparative
511 study employs Nafion[®] drying technologies to reduce or eliminate the water vapor interferences. The use
512 of a chemical (NO) scrubber for UV photometric instruments (such as the 2B Technologies Model 211)
513 is very specific to O₃ and shows a much better response than the catalytic scrubber instruments,
514 performing almost as well as the NO-CL FRM, and has significant potential as a low-interference O₃
515 method. Of the catalytic scrubber photometric instruments those with Nafion[®]-based humidity
516 equilibration (2B Technologies Model 205) perform significantly better than those without (Thermo 49
517 series).

518

519 In areas highly impacted by smoke or for studies focusing on biomass burning plumes, the use of a NO-
520 CL FRM instrument is highly recommended as it was found to be essentially interference-free. These
521 instruments are anchored to absolute O₃ concentrations through the use of certified O₃ calibration sources,

522 many of which are based on UV photometry. The newest generation of commercially-available NO-CL
523 FRM instruments, including that used here (the Teledyne T265), have a built-in drying system to correct
524 for the humidity artifacts that affected earlier generation chemiluminescence instruments (Kleindienst et
525 al., 1993), making remaining interferences negligible compared to other technologies.

526

527 The gas-phase chemical scrubber UV instrument (2B 211), did not perform as well as the FRM under the
528 prescribed grassland burns or chamber experimental conditions tested here, with the high time resolution
529 (1-minute) data showing a much higher degree of variability than the NO-CL FRM instrument. We
530 hypothesize that the main factor driving this divergence between this method and the NO-CL FRM is the
531 dual-cell differential configuration of the instrument, which is not conducive to rapidly changing
532 concentrations in O₃ or other absorbing gases, such as VOCs.

533

534 In smoke-impacted monitoring situations where the use of a UV photometric instrument is still preferred
535 or required, the choice of a monitor with humidity equilibration provides a significant analytical
536 improvement over those monitors without the humidity corrections. In the absence of an instrument with
537 a Nafion[®] tube dryer and in non-regulatory applications, a dryer can be installed before the inlet or
538 measurement cells to reduce the interference as was demonstrated on the final day of the 2018 Missoula
539 chamber burns. This will have the added benefit of reducing positive biases from humidity and reducing
540 equilibration time for calibrations (especially when switching from high humidity ambient air to dry
541 calibration gases).

542 **3.4 Magnitude of Ozone Artifact in Fresh Biomass Burning Plumes Relative to Markers of** 543 **Combustion**

544 It is difficult to estimate an absolute magnitude or correct for the observed O₃ analytical artifact since
545 primary emissions from biomass combustion are highly variable and depend upon the fuel loading, fuel
546 type and condition, phase of the fire, and the burn conditions (Yokelson et al., 1996; Yokelson et al.,
547 1997). However, assuming the interference is driven primarily by VOCs, the artifact should be correlated
548 with the excess CO ($\Delta\text{CO} = \text{CO}_{\text{plume}} - \text{CO}_{\text{background}}$). Because CO_{background} during the prescribed grassland
549 burns was below 200 ppb (relative to typical conditions of >2 ppm in the plume), ΔCO is estimated as the

550 total measured CO concentration. A simplified view of biomass combustion assumes an approximate
551 linear combination of two dominant emission phases, flaming combustion (characterized by emission of
552 highly oxidized compounds, such as CO₂, NO_x, and SO₂), and smoldering combustion (characterized by
553 emission of reduced or mixed oxidation state compounds, such as CO, CH₄, NH₃, H₂S, and most VOCs)
554 (Yokelson et al., 1996; Yokelson et al., 1997). Because the majority of VOCs are in a reduced or mixed
555 oxidation state, they tend to be co-emitting with CO during smoldering combustion, and the VOC
556 concentrations tend to be highly correlated with CO in fresh biomass burning plumes (Yokelson et al.,
557 1996). Scatterplots comparing the FEM instrument artifacts ($\Delta O_{3(UV-C)}$) and CO for the three prescribed
558 grassland burning periods are shown in Fig. 5. Regression statistics of the comparison of $\Delta O_{3(UV-C)}$ and
559 $\Delta O_{3(UV-C-H)}$ with CO and THC for grassland burns are given in Table 4. The magnitude of the artifact
560 (estimated by the slope of the regression line of the CO vs ΔO_3 comparison), in ppb apparent O₃ per ppm
561 CO, ranges between 16 - 24 ppb ppm⁻¹ for the UV-C instrument, and ~~1.5-3.5~~ ppb ppm⁻¹ for the instrument
562 with humidity correction (UV-C-H). It is important to point out that CO, in and of itself, is not considered
563 to be an interfering species in the UV photometric determination of O₃ in that CO absorbs in the infrared
564 (IR). The slight differences in the magnitude of the artifacts (fitted regression slopes) along with the low
565 uncertainty (standard errors) values indicate that the magnitude of the artifact may be influenced by local
566 conditions that make each burn unique. Such conditions might include meteorological conditions, fuel
567 composition, fuel moisture content, and times spent in combustion phase (flaming vs smoldering). Similar
568 to CO, THC_s and NO₂ are indicative of combustion processes and are correlated with ΔO_3 as given in
569 Table 4 and Supplementary Figs. S7 and S8. In terms of THC, the magnitude of the artifact, in ppb
570 apparent O₃ per ppm THC, is significantly higher at ~88 ppb ppm⁻¹ for the UV-C instrument and ~13 ppb
571 ppm⁻¹ for the UV-C-H instrument. Both the prescribed grassland and Missoula chamber burns resulted in
572 what would be considered high PM concentrations (2-50 mg m⁻³). These high PM concentrations
573 however, are not considered to be interfering due to the presence of the inline particle filter assemblies
574 described in Sections 2.2 and 2.6.

575

576 **Table 4: Regression statistics for the ozone artifact (ΔO_3) versus CO and THC for UV photometric**
 577 **instruments without (UV-C) and with (UV-C-H) a Nafion®-based humidity equilibration system**
 578 **during the 2017 prescribed grassland burns.**

Study	Slope (ppb/ppm)	Intercept (ppb)	r ²	n
$\Delta O_{3(UV-C)}$ vs CO				
Mar. 2017 Konza Prairie (KS)	16.46(±0.34) ^a	22.918.53(±6.72) ^b	0.79	679653
Oct. 2017 Sycan Marsh (OR)	24.02(±0.25)	-28.05(±2.73)	0.96	295
Nov. 2017 Konza & Tallgrass Prairies (KS)	23.51(±0.73)	-20.8(±13.03)	0.74	461
$\Delta O_{3(UV-C)}$ vs THC				
Nov. 2017 Konza & Tallgrass Prairies (KS)	87.14(±3.74)	-85.36(±18.63)	0.59	461
$\Delta O_{3(UV-C-H)}$ vs CO				
Mar. 2017 Konza Prairie (KS)	1.46(±0.04)	0.87(±1.03)	0.80	163
Oct. 2017 Sycan Marsh (OR)	2.21(±0.05)	3.44(±0.54)	0.88	296
Nov. 2017 Konza & Tallgrass Prairies (KS)	3.24(±0.09)	-1.17(±1.67)	0.77	461
$\Delta O_{3(UV-C-H)}$ vs THC				
Nov. 2017 Konza & Tallgrass Prairies (KS)	13.27(±0.39)	-14.53(±1.92)	0.75	461
CO-THC vs THC-CO				
Nov. 2017 Konza & Tallgrass Prairies (KS)	0.21(±0.004)	1.55(±0.08)	0.79	461

579 ^aStandard error or uncertainty of the linear regression slope in ppb/ppm

580 ^bStandard error or uncertainty of the linear regression intercept in ppb

581 Since the CO concentrations (from upwind fires) observed at most stationary sites from fire plumes are
 582 usually on the order of one ppm to greater than 10 ppm (Landis et al., 2018), it is reasonable to assume
 583 that O₃ artifacts in the range of 15 ppb to greater than 250 ppb can be observed when employing a UV-C
 584 method. Similarly, O₃ artifacts in the range of 1.5 to above 30 ppb might be observed at smoke-impacted
 585 sites monitoring with UV-C-H methods. As such, Nafion®-based humidity conditioning systems are
 586 highly recommended for use if employing UV photometric methodology for monitoring O₃ in areas
 587 impacted by wildfires or prescribed burns. As stated previously and as seen in Fig. 3 and Table 3, O₃
 588 artifacts were observed during the Missoula chamber 2018 and 2019 burns in both the UV-C and UV-C-
 589 H methods, although reduced compared to the prescribed grassland burns. The presence and magnitude
 590 of the O₃ artifact strongly suggests that smoke generated from fuels typical of forests in the western United
 591 States also result in a measurement interference in UV photometric methods. Since downwind O₃
 592 production in biomass burning plumes is a significant issue in fire impacted regions, having reliable,
 593 interference-free methods is critical for assessing the contribution of wildland fires to ambient O₃ levels.

Formatted Table

Formatted: Superscript

Formatted Table

Formatted: Superscript

Formatted Table

Formatted Table

Formatted Table

Formatted: Superscript

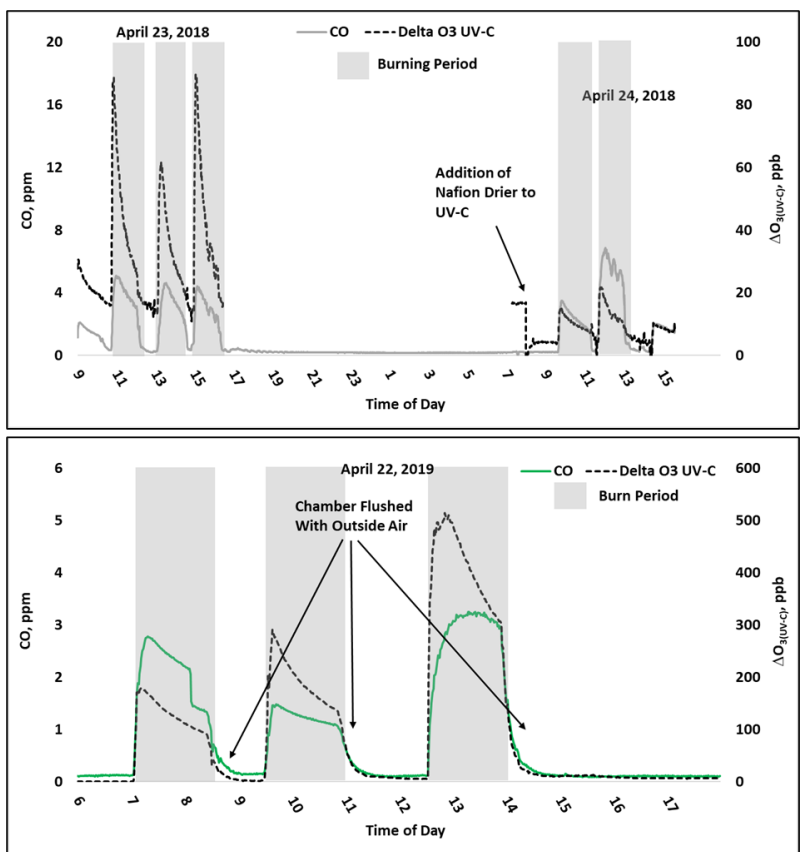
Formatted: Line spacing: single

Formatted: Superscript

594 Figure 6 gives a detailed time series view of $\Delta O_{3(UV-C)}$ and CO from two burn days from 2018 and a single
595 day during 2019. As indicated, $\Delta O_{3(UV-C)}$ and CO appear to be correlated in time but when performing
596 linear regression comparisons of $\Delta O_{3(UV-C)}$ and CO during each years chamber burns as a whole,
597 correlations tend to be poor. We suspect the positive O_3 bias is driven by one or more VOCs (likely
598 oxygenated VOCs). In fresh smoke the excess concentrations of individual VOCs (ΔX), and VOC sums
599 (ΔVOC), tend to be highly correlated with ΔCO (Yokelson et al., 1999; Gilman et al. 2015). The emission
600 ratios of individual VOCs to CO ($\Delta X/\Delta CO$) can vary considerably with combustion conditions such as
601 fuel type and condition (e.g. moisture content and decay state), fuel bed properties, such as bulk density,
602 and the relative mix of flaming and smoldering combustion (Gilman et al. 2015; Koss et al., 2017).
603 Additionally, the response of $\Delta X/\Delta CO$ to burn conditions varies among VOCs. When each burn is
604 considered individually or in groups with similar conditions, the correlations between ΔO_3 , CO, and THC
605 are enhanced. An example of this behavior is shown in Supplementary Fig. S10. For the chamber burns
606 the magnitude of the ozone artifacts in ppb apparent O_3 per ppm CO, ranges between 6 - 210 ppb ppm⁻¹
607 for the individual burns. R^2 and standard error values were consistent with those observed during the
608 prescribed burns (see Table 4). The lack of a consistent relationship between the O_3 artifact and ΔCO
609 across all FSL chamber burns, while observing a good correlation for individual burns, likely reflects the
610 variable response of artifact producing emission(s) to the different combustion conditions of the burns.

611
612 One interesting observation from the data obtained from both the prescribed grassland and chamber burns
613 is the order of magnitude difference in the average and maximum O_3 artifact between the UV-C and the
614 UV-C-H instruments as shown in Table 3. Considering that the prescribed grassland and chamber burns
615 were conducted under dry ($RH < 50\%$) conditions, the size of the difference (as large as hundreds of
616 ppb) cannot be explained purely by the previously observed relative humidity effects on measurements
617 (Leston et al.,
618

Formatted: Superscript



619

620 **Figure 6.** Time series example of USFS chamber burn $\Delta O_3(\text{UV-C})$ and CO concentration results from
 621 April 23-24, 2018 (top) and April 22, 2019 (bottom).

622

623 2005; Wilson et al., 2006), suggesting that the Nafion[®] dryer is directly impacting the concentrations of
 624 other interferents in the sample stream.

625

626 **3.5 Potential Reason for Lower Artifacts with Methods Employing Nafion[®]-based Humidity**
627 **Equilibration**

628 Nafion[®] is a sulfonated tetrafluoroethylene polymer that is highly permeable to water but shows little
629 permeability to many other organic and inorganic species (Mauritz et al., 2004). As a result, Nafion[®]-
630 based drying systems are often used as part of sample preparation or conditioning systems in analytical
631 chemistry to remove water vapor from sample streams prior to sample analysis. Nafion[®] membranes were
632 introduced to some O₃ monitors as a method to address humidity effects observed in UV-C O₃ monitors,
633 particularly when there are rapid changes in relative humidity level (Wilson and Birks, 2006). Humidity
634 can affect the transmission of the UV light through the detection cell and catalytic O₃ scrubbers can
635 modulate the water vapor in the scrubbed channel by acting as a temporary reservoir, resulting in
636 significant positive or negative O₃ interferences during rapid swings in relative humidity Wilson et al.,
637 2006). Adding a Nafion[®]-based equilibration dryer immediately prior to the measurement cells reduces
638 this water vapor interference without affecting O₃ concentrations, and thus significantly reduces the
639 humidity artifacts in UV photometric O₃ instruments.

640

641 Despite the high selectivity of Nafion[®] to water vapor, it does demonstrate partial to complete
642 permeability to various VOC or semivolatile organic compounds. Nafion[®] membranes are highly
643 permeable to alcohols, amines, ketones, and some water-soluble ethers (Baker, 1974), as well as some
644 biogenic oxygenated compounds (Burns et al., 1983). In addition, Nafion[®] membranes have been shown
645 to catalyze the decomposition and rearrangement of monoterpene compounds (Burns et al., 1983).
646 Systematic study of Nafion[®] permeability and reactivity for polar and oxygenated compounds has been
647 limited, with most users of Nafion[®] membranes basing their use on operational testing and confirmation
648 for the targeted use.

649

650 The significant (order of magnitude) reduction in the O₃ artifact with the addition of a Nafion[®]-based
651 dryer to the UV-C suggests that the Nafion[®] dryer is directly impacting the major interfering species
652 which was hypothesized to be VOCs emitted during combustion processes. The species that are
653 responsible for most of the O₃ artifact in UV-C O₃ instruments would have to be permeable through

654 Nafion[®] membranes or reactive with Nafion[®] membranes, be scrubbed by solid-phase, catalytic O₃
655 scrubbers (such as MnO₂ or hopcalite), and would have a significant absorption cross section around 254
656 nm. The absorption cross-section of O₃ around 254 nm is on the order of 10⁻¹⁷ cm² molecule⁻¹ (Molina
657 and Molina, 1986), which means species with absorptions around 10⁻¹⁷ cm² molecule⁻¹ at 254 nm would
658 be potential interfering species. As a class, aromatic VOCs and specifically oxygenated aromatic species
659 (and other polar derivatized species) absorb strongly in this region of the UV spectrum, and their potential
660 permeability through Nafion[®] membranes result in them being likely compounds to interfere in UV-C
661 instruments. As an example, aromatic aldehydes such as o-tolualdehyde and p-tolualdehyde absorbances
662 around 5x10⁻¹⁸ cm² molecule⁻¹ and 4x10⁻¹⁸ cm² molecule⁻¹, respectively (Etzkorn et al., 1999). Both 2,4-
663 dimethylbenzaldehyde and 2,6-dimethylbenzaldehyde have absorption cross sections above 10⁻¹⁷ cm²
664 molecule⁻¹ at 254 nm (El Dib et al., 2008). Baker (1974) found 75% of benzaldehyde was removed by a
665 Nafion[®] membrane, meaning that the Nafion[®] permeability of tolualdehydes and dimethylbenzaldehydes
666 is also likely to be high. In addition, benzaldehyde was almost quantitatively removed by several
667 commercial catalytic O₃ scrubbers, including the Thermo 49i MnO₂ catalytic scrubber (Kleindienst et al.,
668 1993), so similar aldehydes are likely to behave in a similar manner. Therefore, substituted aromatic
669 aldehyde species are one class of compounds that fit the necessary criteria for causing the interference on
670 the UV-C while having a reduced interference on the UV-C-H instrument. Future work examining the
671 potential interferences from different species (or classes of species) on a species or class specific basis
672 are required to confirm this potential mechanism and suggest others.

673 **4 Implications**

674 Wildland fires (wildfires and prescribed fires) emit significant amounts of VOCs and NOx, two important
675 precursors in the photochemical formation of tropospheric O₃. Therefore, it is not surprising that large
676 increases in O₃ are routinely reported at ambient monitoring sites downwind from wildland fires (DeBell
677 et al., 2004; Bytnerowicz et al., 2010; Preisler et al., 2010; Jaffe et al., 2012; Bytnerowicz et al., 2013;
678 Jaffe et al., 2013; Lu et al., 2016; Lindaas et al., 2017; Baylon et al., 2018; Liu et al 2018; McClure and
679 Jaffe, 2018). For example, Buysse et al. (2019) examined regulatory air monitoring data from 18 cities
680 over a five period, and found that July – September exceedances of NAAQS for O₃ were far more common

681 on days with known wildland fire smoke impacts (4.6%) than those without (<0.1%). However, the results
682 of this study suggests caution when interpreting UV photometric method O₃ measurements under
683 conditions of wildfire smoke impact due to the significant positive artifacts that were observed. The
684 analytical artifacts were also shown to be positively correlated with widely used markers of combustion
685 such as CO and THC suggesting that the artifacts arise from photometric measurement interferences by
686 VOCs and further complicating the interpretation of smoke impacted UV photometric O₃ data. As
687 described in section 3.4, it reasonable to assume that O₃ artifacts in the range of a few ppb to greater than
688 250 ppb in addition to actual photochemically formed O₃ can be observed when employing UV
689 photometric methods at sites downwind from fires.

690
691 A detailed example of observed artifacts in the UV photometric method occurred during the 2016 Fort
692 McMurray Horse River wildfire in Alberta, Canada, where elevated “O₃” concentrations were observed
693 at multiple community based air monitoring sites utilizing UV-C instruments in the vicinity of the fire
694 (Landis et al., 2018). Reported “O₃” concentrations reached maximum hourly concentrations in excess of
695 1500 ppb using UV-C methods at night (between 10:00 PM and 5:00 AM local) in the absence of
696 photochemistry and were positively correlated with the combustion markers NO and non-methane
697 hydrocarbon (NMHC). Peaks in O₃ concentration are expected to be negatively correlated with peaks in
698 NO concentration as it rapidly titrates O₃ to NO₂, and the authors hypothesized that UV photometric
699 measurement artifacts may have been responsible for the unexpected observations.

700
701 The findings from this research effort and the observations from ambient studies (Landis et al., 2018)
702 raise concerns that routine regulatory monitoring and wildland fire research study O₃ measurements
703 utilizing UV photometric FEM instruments may be reporting positive measurement artifacts as O₃ during
704 smoke impacted events. Some studies have hypothesized that rapid photochemical processing was
705 responsible for reported elevated O₃ concentrations reported in downwind wildfire plumes (Liu et al.,
706 2017). Since downwind O₃ production in biomass burning plumes is a significant issue in fire impacted
707 regions, having reliable, interference-free methods is critical for assessing the contribution of wildland

708 fires to ambient O₃ levels and developing/validating accurate deterministic air quality models. Air quality
709 researchers and environmental regulators are strongly encouraged to utilize NO-CL FRM O₃ instruments
710 in areas routinely impacted by wildland fire smoke.

711 **4.5 Conclusions**

712 In this study, we compare two different O₃ measurement methods (chemiluminescence and UV
713 photometry) in fresh biomass burning plumes from prescribed grassland fires and during controlled
714 chamber burns. Within the UV photometry category, we look at two different technologies, one using a
715 gas-phase chemical scrubber (NO) and the second using solid phase catalysts to scrub O₃ from analytical
716 reference channels. Among the UV photometric instruments employing solid phase catalytic scrubbers,
717 we evaluated and compared methods that include a Nafion[®]-based humidity equilibration system with
718 those that do not.

719
720 The NO-CL method, recently promulgated as the O₃ FRM, performed well, even in fresh plumes, whereas
721 the UV photometric methods displayed varying degrees of positive measurement artifacts. The UV
722 photometric method employing the dynamic NO gas phase scrubber performed comparably with the NO-
723 CL method but was not well suited to the rapidly varying concentrations of VOCs in the smoke plumes.
724 The catalytic scrubber photometric methods demonstrated positive analytical artifacts that were correlated
725 with CO and THC concentrations (both biomass burning plume indicators). There was a significant
726 difference between the catalytic scrubber UV instruments with and without Nafion[®]-based humidity
727 correction, with the dryer system reducing the positive O₃ artifact by an order of magnitude as compared
728 with the UV photometric method employing no humidity correction. The observed reduction in artifacts
729 cannot be attributed only to elimination of the relative humidity/water vapor interferences and likely result
730 from post-scrubber equilibration or reaction of Nafion[®]-permeable VOCs prior to the measurement cell.
731 The results of this study strongly suggest that careful consideration be given to employed measurement
732 methods when monitoring O₃ concentrations in regions where impacts from biomass burning routinely
733 occur due to the significant impact of potential measurement interferences. In addition to consideration
734 of operating methods containing Nafion[®]-based humidity condition systems, attention should be focused

735 on the scrubbers employed by UV photometric methods and the adverse effects that operation in smoke
736 may have on those scrubbers. Further research is being conducted to evaluate the magnitude of the artifact
737 in the UV photometric method at routine monitoring sites that are often impacted by wildland fire smoke
738 events under the EPA Mobile Ambient Smoke Investigation Capability (MASIC) program (U.S. EPA
739 2019).

740

741 **Data Availability**

742 Datasets related to this manuscript can be found at <https://catalog.data.gov/dataset/epa-sciencehub>.

743

744 **Author Contributions**

745 Russell W. Long served as principal investigator and prepared the manuscript with contributions from all
746 co-authors. Russell W. Long, Andrew Whitehill, Andrew Habel, Maribel Colón, Shawn Urbanski, and
747 Matthew S. Landis performed the prescribed grassland fire and FSL chamber-based data collection and/or
748 analysis. Surender Kaushik performed supervisory review of this research effort and corresponding
749 manuscript.

750

751 **Competing Interests**

752 The authors declare that they have no conflict of interest.

753

754 **Disclaimer**

755 The views expressed in this paper are those of the authors and do not necessarily reflect the views or
756 policies of EPA. It has been subjected to Agency review and approved for publication. Mention of trade
757 names or commercial products do not constitute an endorsement or recommendation for use.

758

759 **Acknowledgements**

760 The EPA through its Office of Research and Development (ORD) funded and conducted this research.
761 We thank Kansas State University, The Nature Conservancy, Konza Prairie Biological Station staff,
762 Sycan March Preserve staff, Tallgrass Prairie National Preserve staff, numerous burn crews, Brian Gullet
763 (EPA), Cortina Johnson (EPA), Melinda Beaver (EPA), Libby Nessley (EPA), and Kyle Digby (Jacobs).

764 **References**

765 [Akagi, S. K., Craven, J. S., Taylor, J. W., McMeeking, G. R., Yokelson, R. J., Burling, I. R., et al.](#)
766 [Evolution of Trace Gases and Particles Emitted by a Chaparral Fire in California. *Atmosph. Chem. Phys.*,](#)
767 [12: 1397-1421, 2012.](#)

768
769 Baker, B. B., Measuring trace impurities in air by infrared spectroscopy at 20 meters path and 10
770 atmospheres pressure, *Am. Ind. Hyg. Assoc. J.*, 35, 735-740, 1974.

771
772 [Baylon, P., Jaffe, D. A., Hall, S. R., Ullmann, K., Alvarado, M. J., & Lefer, B. L.. Impact of Biomass](#)
773 [Burning Plumes on Photolysis Rates and Ozone Formation at the Mount Bachelor Observatory, *J.*](#)
774 [*Geophys. Res.: Atmos.*, 123: 2272–2284, 2018.](#)

775
776 Bertschi, I.; Yokelson, R.J.; Ward, D.E.; Babbitt, R.E.; Susott, R.A.; Goode, J.G.; Hao, W.M., Trace gas
777 and particle emissions from fires in large diameter and belowground biomass fuels, *J. Geophys. Res.*, 108
778 (D13):8472, 2003.

779
780 Boylan, P., Helmig, D., and Park, J.H., Characterization and mitigation of water vapor effects in the
781 measurement of ozone by chemiluminescence with nitric oxide, *Atmos. Meas. Tech.* 7, 1231-1244, 2014.

782
783 Burns, W. F., Tingey, D. T., Evans, R. C., and Bates, E. H., Problems with a Nafion® membrane dryer
784 for drying chromatographic samples, *J. Chromatogr. A*, 269, 1-9, 1983.

785
786 [Buysse, C. E., Kaulfus, A., Nair, U., & Jaffe, D. A., Relationships Between Particulate Matter, Ozone,](#)
787 [and Nitrogen Oxides During Urban Smoke Events in the Western US. *Environ. Sci. Technol.*, 53: 12519-](#)
788 [12528, 2019.](#)

789
790 [Bytnerowicz, A., Cayan, D., Riggan, P., Schilling, S., Dawson, P., Tyree, M., Wolden, L., Tissell, R.,](#)
791 [Preisler, H., Analysis of the Effects of Combustion Emissions and Santa Ana Winds on Ambient Ozone](#)
792 [During the October 2007 Southern California Wildfires, *Atmos. Environ.*, 44: 678-687, 2010.](#)

793
794 [Bytnerowicz, A., Burley, J.D., Cisneros, R., Preisler, H.K., Schilling, S., Schweizer, D., Ray, J., Dulen,](#)
795 [D., Beck, C., Auble, B., Surface Ozone at the Devils Postpile National Monument Receptor Site during](#)
796 [Low and High Wildland Fire Years, *Atmosph. Environ.*, 65: 129-141, 2013.](#)

797
798 Christian, T. J., Kleiss, B., Yokelson, R. J., Holzinger, R., Crutzen, P. J., Hao, W. M., W.M., Saharjo,
799 B.H., Ward, D.E., Comprehensive laboratory measurements of biomass-burning emissions: 2. First
800 intercomparison of open-path FTIR, PTR-MS, and GC- MS/FID/ECD, *J. Geophys. Res.: Atmos.*,
801 109(D2), 2004.
802

803 *DeBell, L. J., Talbot, R. W., Dibb, J. E., Munger, J. W., Fischer, E. V., & Frohking, S. E., A Major*
804 *Regional Air Pollution Event in the Northeastern United States Caused by Extensive Forest Fires in*
805 *Quebec, Canada, *J. Geophys. Res.: Atmos.*, 109(D19): 2004.*
806

807 Dunlea, E., Herndon, S., Nelson, D., Volkamer, R., Lamb, B., Allwine, E., Grutter, M., Ramos Villegas,
808 C., Marquez, C., and Blanco, S., Evaluation of standard ultraviolet absorption ozone monitors in a
809 polluted urban environment, *Atmos. Chem. Phys.*, 6, 3163-3180, 2006.
810

811 El Dib, G., Chakir, A., and Mellouki, A., UV absorption cross-sections of a series of
812 dimethylbenzaldehydes, *J. Phys. Chem. A*, 112, 8731-8736, 2008.
813

814 Etzkorn, T., Klotz, B., Sørensen, S., Patroescu, I. V., Barnes, I., Becker, K. H., and Platt, U., Gas-phase
815 absorption cross sections of 24 monocyclic aromatic hydrocarbons in the UV and IR spectral ranges,
816 *Atmos. Environ.* 33, 525-540, 1999.
817

818 Fiedrich, M., Kurtenbach, R., Wiesen, P., and Kleffmann, J., Artificial O₃ formation during fireworks,
819 *Atmos. Environ.* 165, 57-61, 2017.
820

821 Gilman, J. B., Lerner, B. M., Kuster, W. C., Goldan, P. D., Warneke, C., Veres, P. R., et al., Biomass
822 burning emissions and potential air quality impacts of volatile organic compounds and other trace gases
823 from fuels common in the US. *Atmos. Chem. Phys.*, 15(24), 13915-13938, 2015.
824

825 Grosjean, D., and Harrison, J., Response of chemiluminescence NO_x analyzers and ultraviolet ozone
826 analyzers to organic air pollutants, *Environ. Sci. Tech.*, 19, 862-865, 1985.
827

828 Huntzicker, J. J., and Johnson, R. L., Investigation of an ambient interference in the measurement of
829 ozone by ultraviolet absorption photometry, *Environ. Sci. Tech.*, 13, 1414-1416, 1979.
830

831 *Jaffe, D.A., Wigder, N.L., Ozone Production from Wildfires: A Critical Review, *Atmos. Environ.*, 51: 1-*
832 *10, 2012.*
833

834 *Jaffe, D.A., Wigder, N., Downey, N., Pfister, G., Boynard, A., Reid, S.B., Impact of Wildfires on Ozone*
835 *Exceptional Events in the Western U.S., *Environ. Sci. Technol.*, 47,11065–11072, 2013.*
836

837 Johnson, T., Capel, J., Ollison, W., Measurement of microenvironmental ozone concentrations in
838 Durham, North Carolina, using a 2B Technologies 205 Federal Equivalent Method monitor and
839 interference-free 2B Technologies 211 monitor, *J. Air Waste Manage.*, 64, 360-371, 2014.

840

841 Kleindienst, T. E., Hudgens, E. E., Smith, D. F., McElroy, F. F., and Bufalini, J. J., Comparison of
842 chemiluminescence and ultraviolet ozone monitor responses in the presence of humidity and
843 photochemical pollutants, *Air Waste*, 43, 213-222, 1993.

844

845 Koss, A. R., Sekimoto, K., Gilman, J. B., Selimovic, V., Coggon, M. M., Zarzana, K. J., et al., Non-
846 methane organic gas emissions from biomass burning: identification, quantification, and emission factors
847 from PTR-ToF during the FIREX 2016 laboratory experiment. *Atmos. Chem. Phys.*, 18(5), 3299-3319,
848 2018.

849

850 Landis, M.S., Edgerton, E.S., White, E.M., Wentworth, G.R., Sullivan, A.P., Dillner, A.M., The impact
851 of the 2016 Fort McMurray Horse River Wildfire on ambient air pollution levels in the Athabasca Oil
852 Sands Region, Alberta, Canada. *Sci. Total Environ.*, 618:1665-1676, 2018.

853

854 Landis, M.S., Long, R.W., Krug, J., Colon, M., Vanderpool, R., Habel, A., Urbanski, S., The U.S. EPA
855 Wildland Fire Sensor Challenge: Performance and evaluation of Solver Submitted Multi-Pollutant Sensor
856 Systems. *Atmos. Environ.* In Press.

857

858 Leston, A. R., Ollison, W. M., Spicer, C. W., and Satola, J., Potential interference bias in ozone standard
859 compliance monitoring, *J. Air Waste Manage.*, 55, 1464-1472, 2005.

860

861 Lindaas, J., Farmer, D. K., Pollack, I. B., Abeleira, A., Flocke, F., Roscioli, R., et al., Changes in ozone
862 and precursors during two aged wildfire smoke events in the Colorado Front Range in summer 2015.
863 *Atmos. Chem. Phys.*, 17(17): 10691-10707, 2017.

864

865 Liu, X., Huey, L.G., Yokelson, R.J., Selimovic, V., Simpson, I.J., Müller, M., Jimenez, J.L.,
866 Campuzano-Jost, P., Beyersdorf, A.J., Blake, D.R., Butterfield, Z., Choi, Y., Crouse, J.D.,
867 Day, D.A., Diskin, G.S., Dubey, M.K., Fortner, E., Hanisco, T.F., Hu, W., King, L.E.,
868 Kleinman, L., Meinardi, S., Mikoviny, T., Onasch, T.B., Palm, B.B., Peischl, J., Pollack,
869 I.B., Ryerson, T.B., Sachse, G.W., Sedlacek, A.J., Shilling, J.E., Springston, S., St. Clair,
870 J.M., Tanner, D.J., Teng, A.P., Wennberg, P.O., Wisthaler, A., Wolfe, G.M., Airborne
871 Measurements of Western U.S. Wildfire Emissions: Comparison with Prescribed Burning
872 and Air Quality Implications. *J. Geophys. Res.: Atmos.* 122:6108–6129, 2017.

873

874 Liu, Z., Liu, Y., Murphy, J.P., Maghirang, R., Contributions of Kansas Rangeland Burning to Ambient
875 O₃: Analysis of data from 2001 to 2016. *Sci. Total Environ.*, 618: 1024–1031, 2018.

876

Formatted: Font: Italic

Formatted: Font: Italic

877 Long, R.W., Hall, E., Beaver, M., Duvall, R., Kaushik, S., Kronmiller, K., Wheeler, M., Garvey, S.,
878 Drake, Z., McElroy, F., Performance of the Proposed New Federal Reference Methods for Measuring
879 Ozone Concentrations in Ambient Air, EPA/600/R-14/432, 2014.

880
881 [Lu, X., Zhang, L., Yue, X., Zhang, J., Jaffe, D.A., Stoh, A., Zhao, Y., Shao, J., Wildfire Influences on the](#)
882 [Variability and Trend of Summer Surface Ozone in the Mountainous Western United States, *Atmos.*](#)
883 [*Chem. Phys.*, 16, 14687–14702, 2016.](#)

884
885 Mauritz, K. A., Moore, R.B., State of Understanding of Nafion, Chem. Rev., 104, 10, 4535–4586, 2004.
886

887 [McClure, C. D., & Jaffe, D. A., Investigation of High Ozone Events due to Wildfire Smoke in an Urban](#)
888 [Area. *Atmosp. Environ.*, 194: 146-157, 2018.](#)

889
890 Molina, L.T., Molina, M.J., Absolute Absorption Cross Sections of Ozone in the 185- to 350-nm
891 Wavelength Range, *J. Geophys. Res.; Atmos*, 91 (D13):4719, 1986.

892
893 Ollison, W. M., Crow, W., Spicer, C. W., Field testing of new-technology ambient air ozone monitors, *J.*
894 *Air Waste Manage.*, 63, 855-863, 2013.

895
896 Parrish, D.D., Fehsenfeld, F.C., Methods for gas-phase measurements of ozone, ozone precursors and
897 aerosol precursors, *Atmos. Environ.*, 34, 1921-1957, 2000.

898
899 [Preisler, H.K., Zhong, S., Esperanza, A., Brown, T.J., Bytnerowicz, A., Tarna, L., Estimating Contribution](#)
900 [of Wildland Fires to Ambient Ozone Levels in National Parks in the Sierra Nevada, California, *Environ.*](#)
901 [*Pollut.*, 158: 778-787, 2010.](#)

902
903 Spicer, C. W., Joseph, D. W., and Ollison, W. M., A re-examination of ambient air ozone monitor
904 interferences, *J. Air Waste Manage.*, 60, 1353-1364, 2010.

905
906 [Tong, H. Y., Karasek, F.W., Flame ionization detector response factors for compound classes in](#)
907 [quantitative analysis of complex organic mixtures. *Anal. Chem.*, 56, 2124–2128, 1984.](#)

908
909 Turnipseed, A.A., Andersen, P., Williford, C., Ennis, C., Birks, J., Use of a heated graphite scrubber as a
910 means of reducing interferences in UV-absorbance measurements of atmospheric ozone, *Atmos. Meas.*
911 *Tech.*, 10, 2253–2269, 2017.

912
913 U.S. Environmental Protection Agency (EPA), National Ambient Air Quality Standards for Ozone,
914 *Federal Register*, 80, 206, October 26, 2015.

915
916 U.S. Environmental Protection Agency (EPA), Studies Advance Air Monitoring During Wildfires and
917 Improve Forecasting of Smoke, [https://www.epa.gov/sciencematters/studies-advance-air-monitoring-](https://www.epa.gov/sciencematters/studies-advance-air-monitoring-during-wildfires-and-improve-forecasting-smoke)
918 [during-wildfires-and-improve-forecasting-smoke](https://www.epa.gov/sciencematters/studies-advance-air-monitoring-during-wildfires-and-improve-forecasting-smoke), July 30, 2019.

Formatted: Font: Italic

919
920 Whitehill, A.; George, I.; Long, R.; Baker, K.R.; Landis, M.S., Volatile organic compound emissions
921 from prescribed burning in tallgrass prairie ecosystems. *Atmosphere*, 10, 464, 2019.
922
923 Williams, E. J., Fehsenfeld, F. C., Jobson, B. T., Kuster, W. C., Goldan, P. D., Stutz, J., and McClenny,
924 W. A., Comparison of ultraviolet absorbance, chemiluminescence, and DOAS instruments for ambient
925 ozone monitoring, *Environ. Sci. Technol.*, 40, 5755-5762, 2006.
926
927 Wilson, K. L., and Birks, J. W., Mechanism and elimination of a water vapor interference in the
928 measurement of ozone by UV absorbance, *Environ. Sci. Technol.*, 40, 6361-6367, 2006.
929
930 Yokelson, R.J.; Griffith, D.W.T.; Ward, D.E., Open-path Fourier transform infrared studies of large-scale
931 laboratory biomass fires. *J. Geophys. Res.; Atmos.*, 101(D15):21067-21080, 1996.
932
933 Yokelson, R.J., R Susott, R., Ward, D.E., Reardon, J., Griffith D.W.T., Emissions from smoldering
934 combustion of biomass measured by open-path Fourier transform infrared spectroscopy
935 *J. Geophys. Res.; Atmos.*, 102 (D15), 18865-18877, 1997.
936
937 Yokelson, R. J., Goode, J. G., Ward, D. E., Susott, R. A., Babbitt, R. E., Wade, D. D., et al., Emissions
938 of formaldehyde, acetic acid, methanol, and other trace gases from biomass fires in North Carolina
939 measured by airborne Fourier transform infrared spectroscopy. *J. Geophys. Res.; Atmos.*, 104(D23),
940 30109-30125, 1999.
941
942 Xu, Z., Nie, W., Chi, X., Huang, X., Zheng, L., Xu, Z., Wang, J., Xie, Y., Qi, X., and Wang, X., Ozone
943 from fireworks: Chemical processes or measurement interference?, *Sci. Total Environ.*, 633, 1007-1011,
944 2018.